The Annals of Statistics
2003, Vol. 31, No. 6, 1732–1771

ROTATION SPACE RANDOM FIELDS WITH AN APPLICATION TO fMRI DATA[1]

BY K. SHAFIE, B. SIGAL, D. SIEGMUND AND K. J. WORSLEY

Shahid Beheshti University, *Stanford University*, *Stanford University and McGill University*

Siegmund and Worsley considered the problem of testing for a signal with unknown location and scale in a Gaussian random field defined on $\mathbb{R}^N$. The test statistic was the maximum of a Gaussian random field in an $(N+1)$-dimensional "scale space," N dimensions for location and one dimension for the scale of a smoothing kernel. Siegmund and Worsley used two methods, one involving the expected Euler characteristic of the excursion set and the other involving the volume of tubes, to derive an approximate null distribution. The purpose of this paper is to extend the scale space result to the rotation space random field when $N = 2$, where the maximum is taken over all rotations of the filter as well as scales. We apply this result to the problem of searching for activation in brain images obtained by functional magnetic resonance imaging (fMRI).

1. Introduction. In a variety of applications in astronomy, neural imaging and genetics, one searches a large space of noisy data for a relatively small number of signals in the form of "bumps" in the random noise. This paper builds on the method suggested by Siegmund and Worsley (1995) to detect such signals, with particular attention to fMRI images.

In recent years, very detailed images of the brain, produced by modern sensor technologies, have given the neuroscientist the opportunity to study the functional activation of the brain under different conditions. The main statistical problem is to locate the isolated regions of the brain where activation has occurred (the signal) and separate them from the rest of the brain where no activation can be detected (the noise). To do this, Worsley, Evans, Marrett and Neelin (1992) and Worsley (1994) have shown that the images of the brain can be modeled as a Gaussian random field $X(\mathbf{t})$, where $\mathbf{t} \in \mathbb{R}^N$ is a location vector in the brain $C \subset \mathbb{R}^N$, $N = 3$. Usually, $X_{\max}$, the global maximum of the random field in C, is chosen as the test statistic for detecting signals in the brain.

The images may be spatially smoothed before analysis by convolution with a filter of the form $\sigma^{-N/2}k(\mathbf{t}/\sigma)$ to enhance the signal-to-noise ratio. Often, $k(\mathbf{t})$ is

Received November 2000; revised October 2002.

[1]Supported by the Natural Sciences and Engineering Research Council of Canada, the Fonds pour la Formation des Chercheurs et l'Aide à la Recherche de Québec and the National Science Foundation.

AMS 2000 subject classifications. Primary 60G60, 62M09; secondary 60D05, 52A22.

Key words and phrases. Euler characteristic, differential topology, integral geometry, nonstationary random fields, image analysis.

proportional to a Gaussian density $k(\mathbf{t}) \propto \exp(-\|\mathbf{t}\|^2/2)$. The motivation for this comes from the matched filter theorem of signal processing, which states that a signal added to white noise is best detected by smoothing with a filter whose shape matches that of the signal. A problem is that the scale σ of the signal is usually unknown. It is natural to consider searching over filter scale as well as location, that is, with scale σ varying over a predetermined interval $[\sigma_1, \sigma_2]$. This adds an extra dimension to the search space, called the scale space [see Poline and Mazoyer (1994)]. Siegmund and Worsley (1995) show that $X_{\max}$, the global maximum over all locations in C and all scales σ in $[\sigma_1, \sigma_2]$, is the likelihood ratio statistic for testing for a signal proportional to $\sigma^{-N/2}k(\mathbf{t}/\sigma)$ with unknown location and scale. Using two different approaches—(i) the expected Euler characteristic of the excursion set or (ii) the volume of tubes—they find an approximate P-value of the maximum of the scale space filtered image.

A possible weakness of the scale space random field is a lack of power to detect signals that are not spherically symmetric. In this paper, we extend the scale space result to rotating filters of the form $|\mathbf{S}|^{-1/4}k(\mathbf{S}^{-1/2}\mathbf{t})$, where k is spherically symmetric and $\mathbf{S}$ is now an $N \times N$ positive-definite symmetric matrix that rotates and scales the axes of the filter. Filters of this form add extra dimensions to the search space, which we call rotation space. They are expected to have better power to detect signals that are (approximately) ellipsoidally shaped. A challenging theoretical problem is to deal adequately with the lack of identifiability of the rotation parameter that occurs when the scale parameters are equal.

The concept of scale space has been explored in many image processing tasks [see Lindeberg (1994)] where the filter is usually normalized to preserve the *mean*; that is, the filter at scale $\mathbf{S}$ is $|\mathbf{S}|^{-1/2}k(\mathbf{S}^{-1/2}\mathbf{t})$. In image processing, there is usually no random component, and scale space is used to characterize features in the image that are observed without noise. In our case, likelihood principles (see Section 2) dictate that the filter should be normalized to preserve the *variance* of the filtered white-noise background, which leads to a normalization of $|\mathbf{S}|^{-1/4}$ instead.

The normalization used here is the same as that employed by the continuous wavelet transform [Daubechies (1992)], where the filter or mother wavelet is usually chosen so that $\int k(\mathbf{t})\,d\mathbf{t} = 0$, as well as $\int k(\mathbf{t})^2\,d\mathbf{t} = 1$. The main difference is that the wavelet transform seeks to *represent* the image at different scales; here the aim is to *detect* a localized image increase at an unknown scale and rotation.

The organization of the paper is as follows. In Section 2, we review the scale space random field and introduce the rotation space random field. In Section 3, we introduce the Euler characteristic (EC) approach to making inference about localized signals in these random fields. In Section 4, we introduce a different parameterization of the rotation space field, which we then study from the viewpoint of the volume of tubes. Approximate P-values obtained by the tubes method are shown numerically to be comparable to those obtained by the EC method.

Although we have used two different methods with two slightly different parameterizations, there is strong evidence to suggest that these two methods should yield the same P-value approximations, at least to the first few terms in the threshold x. The evidence for this comes from Takemura and Kuriki (2002) who show that if the random field has a terminating Karhunen–Loève expansion then the EC approach and the tubes approach always give the same answer. In our case (and most interesting cases), the expansion does not terminate, so the agreement between the two approaches is still an open question. To illustrate the different approaches, we use the EC approach with one parameterization and the tubes method with another.

Finally, the power of the rotation space statistic is discussed in Section 5 and is compared to the power of the scale space statistic. In Section 6, we apply the rotation space methods to an fMRI data set. Section 7 contains some concluding remarks. Lengthy technical derivations are given in two appendixes.

2. Scale space and rotation space random fields. Let k be an N-dimensional kernel such that

$$\int k^2(\mathbf{t})\,d\mathbf{t} = 1.$$

A common choice is the Gaussian kernel:

$$k(\mathbf{t}) = \pi^{-N/4}\exp(-\|\mathbf{t}\|^2/2). \tag{1}$$

The Gaussian *scale space* random field is defined as

$$X(\mathbf{t},\sigma) = \sigma^{-N/2}\int k[\sigma^{-1}(\mathbf{h}-\mathbf{t})]\,dZ(\mathbf{h}),$$

where $Z(\mathbf{h})$ is a Gaussian random field defined on a subset of $\mathbb{R}^N$ and σ is a positive constant.

A justification for working on Gaussian scale space random fields, which also serves to motivate the rotation space random field of the following section, is as follows. Assume the random field $Z(\mathbf{t})$, $\mathbf{t}\in\mathbb{R}^N$, satisfies

$$dZ(\mathbf{t}) = \xi\sigma_0^{-N/2}k[\sigma_0^{-1}(\mathbf{t}-\mathbf{t}_0)]\,d\mathbf{t} + dW(\mathbf{t}),$$

where $\mathbf{t}_0\in C\subset\mathbb{R}^N$, $\xi\geq 0$ and $\sigma_0>0$ are fixed values and W is an N-dimensional Brownian sheet. The unknown parameter $(\xi,\mathbf{t}_0,\sigma_0)$ represents the amplitude, location and scale of a signal added to the noise $dW(\mathbf{t})$. In other words, the shape of the signal in $dZ(\mathbf{t})$ matches the shape of the filter k. Models of this form have been used in different scientific contexts, for example, in the study of human brain function via positron emission tomography [Worsley, Evans, Marrett and Neelin (1992) and Worsley (1994)], in functional magnetic resonance imaging [Worsley (2001)] and for geographical clustering of disease incidences [Rabinowitz (1994)].

Now, for testing the hypothesis of no signal, that is, $\xi = 0$, consider the test statistic that rejects for large positive values of

$$X_{\max} = \max_{(\mathbf{t},\sigma)\in C\times[\sigma_1,\sigma_2]} X(\mathbf{t},\sigma).$$

It can be shown [see Siegmund and Worsley (1995)] that the log-likelihood function is

$$\xi X(\mathbf{t},\sigma) - \xi^2/2,$$

so the test defined by $X_{\max}$ is the likelihood ratio test for testing $\xi = 0$.

We now extend the concept of the scale space random field to the rotation space random field, which is obtained by rotating as well as scaling the smoothing filter. Using this rotation space random field should increase the sensitivity of the test statistic in detecting ellipsoidal-shaped signals that might be missed by a circular-shaped filter.

The Gaussian *rotation space* random field is defined as

$$X(\mathbf{t},\mathbf{S}) = \det(\mathbf{S})^{-1/4} \int k[\mathbf{S}^{-1/2}(\mathbf{h}-\mathbf{t})]\, dZ(\mathbf{h}),$$

where k is spherically symmetric and $\mathbf{S}$ is an $N \times N$ symmetric positive-definite matrix. The same likelihood-based argument as above for working on the scale space random field justifies working on the rotation space random field. Assume the random field $Z(\mathbf{t})$, $\mathbf{t} \in \mathbb{R}^N$, satisfies

$$dZ(\mathbf{t}) = \xi \det(\mathbf{S}_0)^{-1/4} k[\mathbf{S}_0^{-1/2}(\mathbf{t}-\mathbf{t}_0)]\, d\mathbf{t} + dW(\mathbf{t}), \tag{2}$$

where $\mathbf{S}_0$ is a member of a fixed parameter set Q of positive-definite matrices. The unknown parameter $(\xi, \mathbf{t}_0, \mathbf{S}_0)$ represents the amplitude, location, orientation and scale of the signal and $dW(\mathbf{t})$ represents noise. The test statistic that rejects for large positive values of

$$X_{\max} = \max_{(\mathbf{t},\mathbf{S})\in C\times Q} X(\mathbf{t},\mathbf{S})$$

is the likelihood ratio test for testing the hypothesis of no signal, that is, $\xi = 0$.

In this paper, we consider two parameter sets, denoted by Q and Q^*, as search regions for the 2×2 positive-definite matrix $\mathbf{S}$. These are shown schematically in Figure 1. For Q, both eigenvalues are in a fixed interval; for Q^*, one eigenvalue is in a fixed interval, and the ratio of the two eigenvalues is in another fixed interval. As explained in Section 1, we will use two different approaches for the two different parameterizations: the Euler characteristic approach for Q (Section 3) and the tubes approach for Q^* (Section 4). The choice is arbitrary—we expect both methods to give very similar results on the same parameterization.

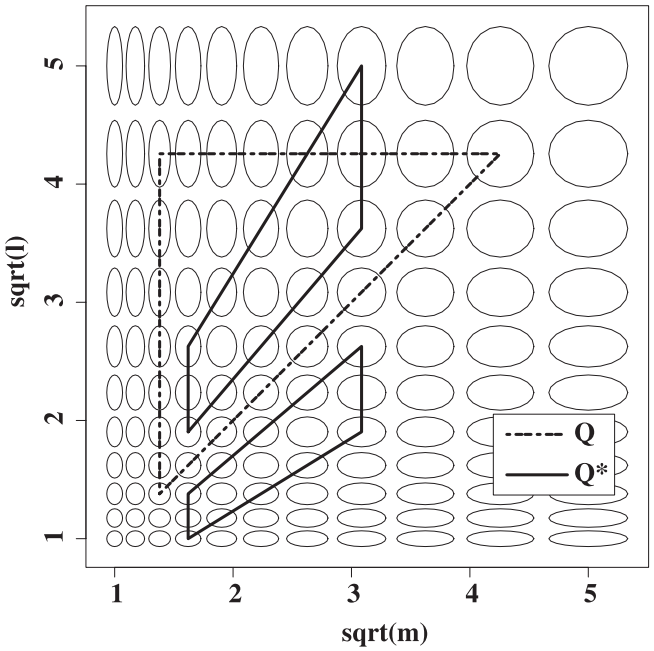

FIG. 1. *Two-dimensional* ($N = 2$) *examples of the two types of rotation space search regions* Q *and* Q^* *for* $\mathbf{S}$ *shown as contours of the unrotated filter. The axes are the square roots of the two eigenvalues* l *and* m *of* $\mathbf{S}$.

3. The Euler characteristic approach. In this paper, we are primarily concerned with finding the P-value of $X_{\max}$. A very good approximation is to use the expectation of the EC of the *excursion set* of the random field inside the search region for the maximum [Adler (1981)]. Specifically,

$$P\{X_{\max} \geq x\} \approx \mathrm{E}[\chi(A_x)],$$

where χ denotes the EC and the excursion set A_x is the set of points in the search region where the random field exceeds the threshold x. The idea behind the success of this approach is that for high thresholds the "handles" and "holes" in the excursion set tend to disappear, and the EC counts the number of connected components of the excursion set. For even higher thresholds, near the maximum, the excursion set contains at most one component, so the EC takes the value 1 if the maximum is above x and 0 if it is below. Hence, the expected EC should accurately approximate the probability that the maximum exceeds x. The appeal of this approach is that in many cases we can obtain an *exact* closed-form expression for $\mathrm{E}[\chi(A_x)]$ for *all* thresholds. Moreover, this closed-form expression typically gives a very good approximation to the P-value of the maximum for search regions of almost any size or shape [see Adler (2000)].

There are two main technical challenges to using the EC method. The first is to find a *point set representation* for the EC using either Morse theory or the

Hadwiger recursive definition, so that the EC can be represented as the integral of this point set representation over the interior and boundary of the search region. The second step is to evaluate the resulting rather complicated expectations involving the random field and its first two derivatives. The calculations in this second step, in the case of the rotation space random field, are so complicated that we have used the computer algebra package MAPLE to produce the results [see Shafie (1998) and www.math.mcgill.ca/shafie]. For the scale space random field, a general result can be found by hand [Siegmund and Worsley (1995) and Worsley (2001)], and for comparison with the rotation space results yet to come, we now give those results.

3.1. *Scale space.*

3.1.1. *Point set representation.* The excursion set of the scale space random field is

$$A_x = \{(\mathbf{t}, \sigma) \in C \times [\sigma_1, \sigma_2] : X(\mathbf{t}, \sigma) \geq x\}.$$

Let $\dot{\mathbf{X}}_\mathbf{t} = \partial X/\partial \mathbf{t}$, $\ddot{\mathbf{X}}_\mathbf{t} = \partial^2 X/\partial \mathbf{t}\, \partial \mathbf{t}'$ and $\mathbf{c}$ be the inside curvature matrix of ∂C. For a fixed σ, we denote the gradient vector of X in the direction of the inside normal to ∂C by $\dot{X}_\perp$ and the gradient $(N-1)$-vector in the tangent plane to ∂C by $\dot{\mathbf{X}}_\mathrm{T}$. In addition, let $\dot{X}_\sigma = \partial X/\partial \sigma$ and $\dot{X}_\sigma^+ = \dot{X}_\sigma$ $(\dot{X}_\sigma > 0)$. If $X(\mathbf{t}, \sigma)$ satisfies the regularity conditions given by Adler (1981), Theorem 5.2.2, then

$$\begin{aligned}
&\mathrm{E}[\chi(A_x)] \\
&\quad = \int_C \int_{\sigma_1}^{\sigma_2} \mathrm{E}[\dot{X}_\sigma^+ \det(-\ddot{\mathbf{X}}_\mathbf{t}) | \dot{\mathbf{X}}_\mathbf{t} = \mathbf{0}, X = x] \phi(\mathbf{0}, x)\, d\mathbf{t}\, d\sigma \\
&\qquad + \int_C \left[\mathrm{E}[(X \geq x) \det(-\ddot{\mathbf{X}}_\mathbf{t}) | \dot{\mathbf{X}}_\mathbf{t} = \mathbf{0}] \theta(\mathbf{0})\right]_{\sigma=\sigma_1} d\mathbf{t} \\
&\qquad + \int_{\partial C} \int_{\sigma_1}^{\sigma_2} \mathrm{E}[\dot{X}_\sigma^+ (\dot{X}_\perp < 0) \det(-\ddot{\mathbf{X}}_\mathrm{T} - \dot{X}_\perp \mathbf{c}) | \dot{\mathbf{X}}_\mathrm{T} = \mathbf{0}, X = x] \\
&\qquad\qquad \times \phi_\mathrm{T}(\mathbf{0}, x)\, d\sigma\, d\mathbf{t} \\
&\qquad + \int_{\partial C} \left[\mathrm{E}[(X \geq x)(\dot{X}_\perp < 0) \det(-\ddot{\mathbf{X}}_\mathrm{T} - \dot{X}_\perp \mathbf{c}) | \dot{\mathbf{X}}_\mathrm{T} = \mathbf{0}] \theta_\mathrm{T}(\mathbf{0})\right]_{\sigma=\sigma_1} d\mathbf{t},
\end{aligned} \tag{3}$$

where $\phi(\cdot, \cdot)$, $\theta(\cdot)$, $\phi_\mathrm{T}(\cdot, \cdot)$ and $\theta_\mathrm{T}(\cdot)$ are the densities of $(\dot{\mathbf{X}}_\mathbf{t}, X)$, $\dot{\mathbf{X}}_\mathbf{t}$, $(\dot{\mathbf{X}}_\mathrm{T}, X)$ and $\dot{\mathbf{X}}_\mathrm{T}$, respectively.

3.1.2. *Expected Euler characteristic.* For the second step, Worsley (2001) evaluates this expectation for any number of dimensions N, but for comparison with our later rotation space results, we just give the result for $N = 2$. Let $\dot{\mathbf{k}}(\mathbf{h}) = \partial k(\mathbf{h})/\partial \mathbf{h}$,

$$\beta \mathbf{I} = \int \dot{\mathbf{k}}(\mathbf{h}) \dot{\mathbf{k}}'(\mathbf{h})\, d\mathbf{h}, \qquad \kappa = \int [\mathbf{h}' \dot{\mathbf{k}}(\mathbf{h}) + (N/2) k(\mathbf{h})]^2\, d\mathbf{h}.$$

For a Gaussian kernel (1), $\beta = 1/2$ and $\kappa = N/2$. Let $r = \sigma_1/\sigma_2$, $\phi(x) = \exp(-x^2/2)/\sqrt{(2\pi)}$ and $\Phi(x) = \int_{-\infty}^{x} \phi(z)\,dz$. Then

$$\begin{aligned}
\mathrm{E}[\chi(A_x)] &= |C|\beta\sigma_1^{-2}\{\kappa^{1/2}(2\pi)^{-1/2}(1-r^2)(x^2-1+1/\kappa)/2 + (1+r^2)x/2\} \\
&\quad \times \phi(x)/(2\pi) \\
&\quad + |\partial C|\beta^{1/2}\sigma_1^{-1}\{\kappa^{1/2}(2\pi)^{-1/2}(1-r)x/2 + (1+r)/4\} \\
&\quad \times \phi(x)/(2\pi)^{1/2} \\
&\quad + \chi(C)\{[1-\Phi(x)] - \kappa^{1/2}(2\pi)^{-1/2}\log r\phi(x)\}.
\end{aligned} \tag{4}$$

3.2. *Rotation space.* Turning now to the rotation space random field, we first define the search region. Introducing the rotation filter adds $N(N+1)/2 - 1$ dimensions to the search space. In general, it is complicated to find the expectation of the EC for such a high-dimensional nonstationary random field, so from now on we consider the simplest case $N = 2$. We assume that the rotation parameter $\mathbf{S} = \left(\begin{smallmatrix} a & c \\ c & b \end{smallmatrix}\right)$ of the random field is restricted to positive-definite matrices with eigenvalues limited to the range $[\sigma_1^2, \sigma_2^2]$. The set Q' of such matrices, embedded in $\mathbb{R}^3$, is the union of two cones as shown in Figure 2.

To simplify the calculation, we reparameterize Q' and write

$$\mathbf{S} = \begin{bmatrix} a & c \\ c & b \end{bmatrix} = \begin{bmatrix} \cos\theta & -\sin\theta \\ \sin\theta & \cos\theta \end{bmatrix} \begin{bmatrix} l & 0 \\ 0 & m \end{bmatrix} \begin{bmatrix} \cos\theta & \sin\theta \\ -\sin\theta & \cos\theta \end{bmatrix},$$

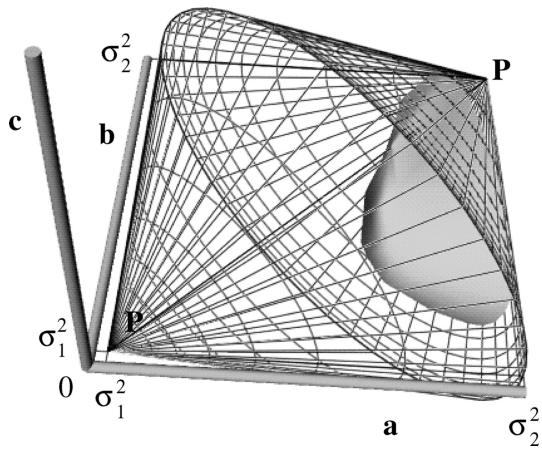

FIG. 2. *Rotation parameter space Q' for $\mathbf{S} = [(a, c)'(c, b)']$ as the union of two cones with common axes along the line $a = b$ (PP). The eigenvalues l and m of $\mathbf{S}$ are in the interval $[\sigma_1^2, \sigma_2^2]$. An example of the excursion set at a single pixel is added (blob at top right).*

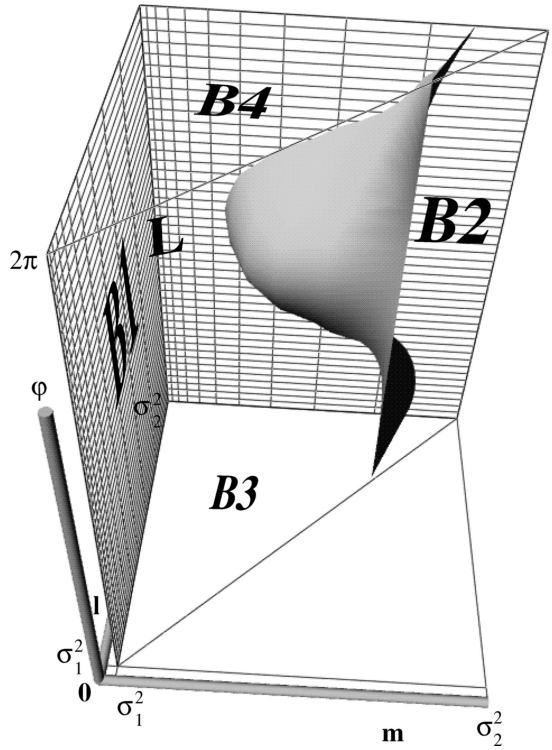

FIG. 3. *Same rotation space as in Figure* 2 *but reparameterized in terms of eigenvalues* $l \geq m \in [\sigma_1^2, \sigma_2^2]$ *and twice the rotation angle* $\varphi \in [0, 2\pi]$, *now denoted by* Q. *The same example of the excursion set at a single pixel is added* (*blob at top right*).

where the eigenvalues l and m are in $[\sigma_1^2, \sigma_2^2]$. Rewriting $\mathbf{S}$ in terms of $\varphi = 2\theta$, we have

$$\mathbf{S} = \begin{bmatrix} (l+m)/2 + ((l-m)/2)\cos\varphi & ((l-m)/2)\sin\varphi \\ ((l-m)/2)\sin\varphi & (l+m)/2 - ((l-m)/2)\cos\varphi \end{bmatrix}.$$

In this section, we use $\mathbf{s} = (l, m, \varphi)$ instead of $\mathbf{S}$ as the parameter of rotation space. Then the domain of the values for $\mathbf{s}$ can be considered as

$$Q = \{(l, m, \varphi) : \sigma_1^2 \leq m \leq l \leq \sigma_2^2,\ 0 \leq \varphi \leq 2\pi\}.$$

The set Q is shown in Figure 3. Our aim is to derive $\mathrm{E}[\chi(A_x)]$, where

$$A_x = \{(\mathbf{t}, \mathbf{s}) \in C \times Q : X(\mathbf{t}, \mathbf{s}) \geq x\}.$$

3.2.1. *Point set representation.* The first step is to find the point set representation for the EC of A_x and take its expectation. As for scale space, we partition $C \times Q$ into different pieces and obtain the contribution of each piece to the EC of the excursion set. Then, using the additivity property of the EC and a generalized

form of (3), we can obtain the expected EC of the excursion set. In partitioning the search set, we face another problem: that the rotation space random field X has some irregular behavior on $P = \{(l, m, \varphi) : l = m\}$. On this set, the random field X is a constant function of φ. Going back to the original rotation space, the union of two cones Q', the set P is the image of P', the rotation axis of Q'. The rotation space random field on this axis is equivalent to a scale space random field. To solve this irregularity, consider the following. We take away the rotation axis of Q' and unfold the rest of Q' to get $Q \setminus P$ and then map the line P' to P. Then we consider the contribution of the image of P', P, to the EC of the excursion set separately. The same kind of argument that enables us to separate a part of the search set has been used in the astrophysics literature [see Gott et al. (1990)].

For simplicity in notation, we henceforth denote the set $Q \setminus P$ by Q and proceed by partitioning the rest of the search set as $C \times Q = (C^\circ \times Q^\circ) \cup (\partial C \times Q^\circ) \cup (C \times \partial Q) \cup (\partial C \times \partial Q)$, where "$\circ$" denotes the interior of a set. In turn, the boundary of Q itself can be partitioned as

$$\partial Q = B_1 \cup B_2 \cup L \cup B_3 \cup B_4, \tag{5}$$

where

$$\begin{aligned}
L &= \{(l, m, \varphi) : l = \sigma_2^2,\ m = \sigma_1^2,\ 0 < \varphi < 2\pi\},\\
B_1 &= \{(l, m, \varphi) : \sigma_1^2 \le l \le \sigma_2^2,\ m = \sigma_1^2,\ 0 < \varphi < 2\pi\},\\
B_2 &= \{(l, m, \varphi) : l = \sigma_2^2,\ \sigma_1^2 \le m \le \sigma_2^2,\ 0 < \varphi < 2\pi\},\\
B_3 &= \{(l, m, \varphi) : \sigma_1^2 \le m \le l \le \sigma_2^2,\ \varphi = 0\},\\
B_4 &= \{(l, m, \varphi) : \sigma_1^2 \le m \le l \le \sigma_2^2,\ \varphi = 2\pi\}.
\end{aligned}$$

A diagram of the above partition is shown in Figure 3. We obtain the contribution of P and of each component of the partition of ∂Q in Appendix A.

3.2.2. *Expected Euler characteristic.* The second step is to evaluate the expected point set representation just found. To do this, we need to have the joint distribution of X and its first two derivatives. This distribution can be obtained by using derivatives of $\mathrm{Cov}[X(\mathbf{t}_1, \mathbf{S}_1), X(\mathbf{t}_2, \mathbf{S}_2)]$. We have

$$\begin{aligned}
&\mathrm{Cov}[X(\mathbf{t}_1, \mathbf{S}_1), X(\mathbf{t}_2, \mathbf{S}_2)]\\
&\quad = \det(\mathbf{S}_1\mathbf{S}_2)^{-1/4} \int k[\mathbf{S}_1^{-1/2}(\mathbf{h} - \mathbf{t}_1)] k[\mathbf{S}_2^{-1/2}(\mathbf{h} - \mathbf{t}_2)]\, d\mathbf{h}\\
&\quad = \det(\mathbf{S}_1\mathbf{S}_2)^{-1/4} \int k[\mathbf{S}_1^{-1/2}(\mathbf{h} + \mathbf{t}_2 - \mathbf{t}_1)] k[\mathbf{S}_2^{-1/2}\mathbf{h}]\, d\mathbf{h}.
\end{aligned}$$

This shows that, for a fixed value of $\mathbf{S}$, $X(\mathbf{t}, \mathbf{S})$ is stationary in $\mathbf{t}$, but $X(\mathbf{t}, \mathbf{S})$ is not stationary in $(\mathbf{t}, \mathbf{S})$. When $k(\mathbf{t})$ is the Gaussian kernel, the covariance function

simplifies to

$$\begin{aligned}&\operatorname{Cov}[X(\mathbf{t}_1,\mathbf{S}_1),X(\mathbf{t}_2,\mathbf{S}_2)]\\&\quad=2^{N/2}\frac{|\mathbf{S}_1|^{1/4}|\mathbf{S}_2|^{1/4}}{|\mathbf{S}_1+\mathbf{S}_2|^{1/2}}\exp\bigl(-(\mathbf{t}_1-\mathbf{t}_2)'(\mathbf{S}_1+\mathbf{S}_2)^{-1}(\mathbf{t}_1-\mathbf{t}_2)/2\bigr).\end{aligned}$$

Note that in the case of the Gaussian kernel there are functional relationships between different derivatives of the rotation space random field $X(\mathbf{t},\mathbf{S})$. Let

$$\dot{\mathbf{X}}_{\mathbf{S}}=\partial X/\partial\mathbf{S}=\begin{bmatrix}\partial X/\partial\mathbf{S}_{11} & \partial X/\partial\mathbf{S}_{12}\\ \partial X/\partial\mathbf{S}_{12} & \partial X/\partial\mathbf{S}_{22}\end{bmatrix}$$

and $\ddot{\mathbf{X}}_{\mathbf{t}}=\partial^2X/\partial\mathbf{t}\,\partial\mathbf{t}'$. Using the heat equation, we can prove that

$$\dot{\mathbf{X}}_{\mathbf{S}}(\mathbf{t},\mathbf{S})=2^{N/2-2}\pi^{N/4}\bigl(2\mathbf{S}^{-1}-\operatorname{diag}(\mathbf{S}^{-1})\bigr)X(\mathbf{t},\mathbf{S})+\ddot{\mathbf{X}}_{\mathbf{t}}(\mathbf{t},\mathbf{S}).$$

As a consequence, it would not be a surprise to see later that some of the conditional distributions are singular.

For simplicity of notation, derivatives of X with respect to t_i will be denoted by dot notation with a subscript i, $i=1,2$. Derivatives with respect to l, m and φ will be denoted by subscripts l, m and φ. To calculate the expectation of the EC, we need to have the distribution of $\mathbf{Y}=(X,\dot{X}_\varphi,\dot{\mathbf{X}}_{12lm},\ddot{\mathbf{X}}_{12lm})$ at a fixed point $(\mathbf{t},\mathbf{s})$, where $\ddot{\mathbf{X}}_{12lm}$ is arranged in the same way that the *vech* operator arranges symmetric matrices [see Searle (1982)]. We know $\mathbf{Y}$ has a multivariate Gaussian distribution with zero mean. The covariance matrix of $\mathbf{Y}$ is obtained by taking suitable derivatives of $\operatorname{Cov}[\mathbf{X}(\mathbf{t}_1,\mathbf{s}_1),\mathbf{X}(\mathbf{t}_2,\mathbf{s}_2)]$ then setting $\mathbf{t}_1=\mathbf{t}_2$ and $\mathbf{s}_1=\mathbf{s}_2$.

The algebra involved in taking these derivatives for a general kernel is very complicated. We decided to choose the Gaussian kernel as the kernel of the rotation space random field. We used the computer algebra program MAPLE to derive the covariance matrix for the Gaussian kernel, although our MAPLE code works for any kernel (see www.math.mcgill.ca/shafie). For the Gaussian kernel, we get

$$\operatorname{Var}(\mathbf{Y})=\begin{bmatrix}1 & 0 & \mathbf{0} & -\operatorname{Var}(\dot{\mathbf{X}}_{12lm})\\ 0 & (l-m)^2/(16lm) & \mathbf{0} & \operatorname{Cov}(\dot{X}_\varphi,\ddot{\mathbf{X}}_{12lm})\\ \mathbf{0} & \mathbf{0} & \operatorname{Var}(\dot{\mathbf{X}}_{12lm}) & \operatorname{Cov}(\dot{\mathbf{X}}_{12lm},\ddot{\mathbf{X}}_{12lm})\\ -\operatorname{Var}(\dot{\mathbf{X}}_{12lm})' & \operatorname{Cov}(\dot{X}_\varphi,\ddot{\mathbf{X}}_{12lm})' & \operatorname{Cov}(\dot{\mathbf{X}}_{12lm},\ddot{\mathbf{X}}_{12lm})' & \operatorname{Var}(\ddot{\mathbf{X}}_{12lm})\end{bmatrix}.$$

For a detailed evaluation of the elements of $\operatorname{Var}(\mathbf{Y})$, see Shafie (1998).

Another complication in obtaining the expected EC is the calculation of the expectation of the determinant of submatrices of $\ddot{\mathbf{X}}_{12lm}$. From Adler (1981), Lemma 5.3.1, it is evident that these expectations depend on the elements of the conditional covariance and mean of $\ddot{\mathbf{X}}_{12lm}$ given $(X,\dot{\mathbf{X}})$. But, unlike the stationary case, the elements of this covariance matrix are not a symmetric function of the indices $(1,2,l,m)$ [see Adler (1981), page 109]. So to obtain the expectation of the random determinants, we used MAPLE. The final result is the following theorem.

THEOREM 1. *For the rotation space random field with a Gaussian kernel, we have*

$$
\begin{aligned}
&\mathrm{E}[\chi(A_x)] \\
&\quad = |C|\frac{\sqrt{2}}{\sigma_1^2}\Bigg\{-\frac{((\log r)(1+r^2)+(1-r^2))x^4}{128\pi^{3/2}} - \frac{(\log r)(1-r^2)x^3}{64\pi} \\
&\qquad\qquad + \frac{((2\pi+15)(1-r^2)+7(\log r)(1+r^2))x^2}{128\pi^{3/2}} \\
&\qquad\qquad + \frac{(2\sqrt{2}(1+r^2)+3(\log r)(1-r^2))x}{32\pi} - \frac{(\pi+2)(1-r^2)}{32\pi^{3/2}}\Bigg\}\phi(x) \\
&\qquad + |\partial C|\frac{1}{\sigma_1}\Bigg\{\int_0^{(1-r^2)^{1/2}} f(t)\,dt \\
&\qquad\qquad + g + \left[\frac{\sqrt{2}}{8\pi}(r-1)x + \frac{1}{8\sqrt{\pi}}(r+1)\right]\Bigg\}\phi(x) \\
&\qquad + \chi(C)\frac{\sqrt{2}}{8}\Bigg\{\Bigg[\frac{(2r(\log r)-r^2+1)x^2}{2\sqrt{\pi}r} - \frac{(2r-r^2-1)x}{r} \\
&\qquad\qquad + \frac{-5r(\log r)+(\pi-1)(1-r^2)}{\sqrt{\pi}r}\Bigg]\phi(x) \\
&\qquad\qquad + 1-\Phi(x)\Bigg\},
\end{aligned}
\tag{6}
$$

where

$$
\begin{aligned}
f(t) = \frac{\sqrt{2}}{32\pi^2}\Bigg\{\Bigg[&\left(\frac{t^3}{t'^3} - \frac{rt^3}{t'^4}\right)x^3 + \left(\frac{\sqrt{\pi}t^3}{t'^3} - \frac{\sqrt{\pi}rt^3}{t'^6}\right)x^2 \\
&+ \left(\frac{-8+6t^2+5t^4}{t'^3t} - \frac{(8-6t^2-5t^4)r}{t'^4}\right)x \\
&+ \frac{(4-2t^2-3t^4)\sqrt{\pi}}{t'^3t} + \frac{(-4+6t^2+t^4)\sqrt{\pi}r}{t'^6}\Bigg]E(t) \\
&+ \Bigg[\left(-\frac{2(4-t^2)r}{tt'} + \frac{2(4-5t^2+2t^4)r)}{tt'^4}\right)x \\
&- \frac{4\sqrt{\pi}}{tt'} + \frac{4\sqrt{\pi}r}{tt'^2}\Bigg]K(t)\Bigg\},
\end{aligned}
$$

$$
\begin{aligned}
g = \frac{\sqrt{2}}{32\pi^{3/2}r}\big[&4r^2K[(1-r^2)^{1/2}] \\
&- \big((1-r^2)\sqrt{\pi}x + 2(1+r^2)\big)E[(1-r^2)^{1/2}]\big],
\end{aligned}
$$

$t' = (1 - t^2)^{1/2}$ and $K(\cdot)$ and $E(\cdot)$ are complete elliptic integrals of the first and second kinds, respectively.

The elliptic integrals are defined by $K(y) = \int_0^{\pi/2}(1 - y^2 \sin^2\theta)^{-1/2}\,d\theta$ and $E(y) = \int_0^{\pi/2}(1 - y^2 \sin^2\theta)^{1/2}\,d\theta$ and are easily evaluated numerically [cf. Abramowitz and Stegun (1964)]. If only moderate accuracy is required, a simple approximation is obtained by expanding the integrands as power series in y and integrating term by term.

A simple example of (6) as a function of the threshold level x when C is a circle of radius 50 and $[\sigma_1^2, \sigma_2^2] = [2, 50]$ is drawn in Figure 4. Note that the expected EC approaches $\chi(C) = 1$ as $x \to -\infty$. To find approximate level α critical thresholds for testing the existence of a signal using $X_{\max}$, we can equate $\mathrm{E}[\chi(A_x)]$ to α and solve for x. For the purpose of comparison, these critical values at the $\alpha = 0.05$ level, as a function of the radius of the circle C for rotation space, scale space [from (4)] and two different values of fixed scale [(4) with $\sigma_1 = \sigma_2$] are plotted in Figure 5. As we can see from this plot, the critical values for rotation space are somewhat larger than those of scale space and fixed scales due to searching over a bigger set.

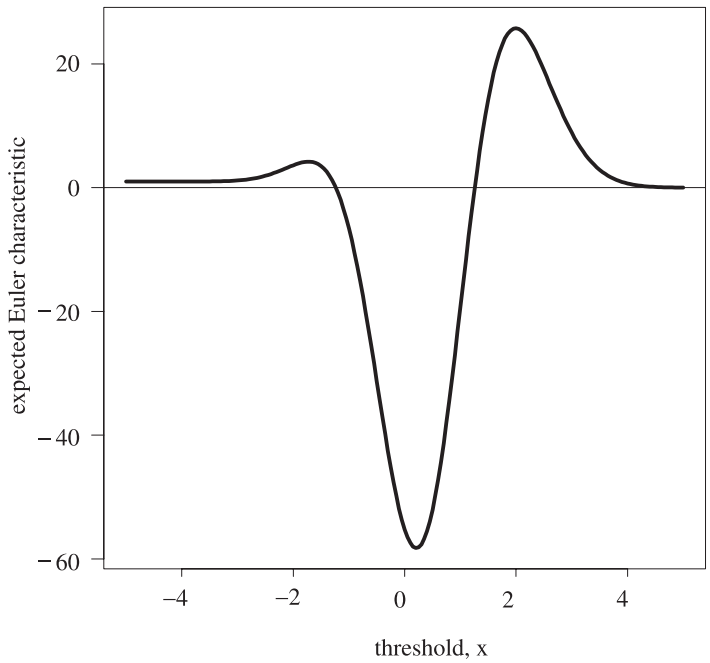

FIG. 4. *Expectation of the Euler characteristic (EC) when the search region C is a circle of radius 50 and $[\sigma_1^2, \sigma_2^2] = [2, 50]$, as a function of the threshold x.*

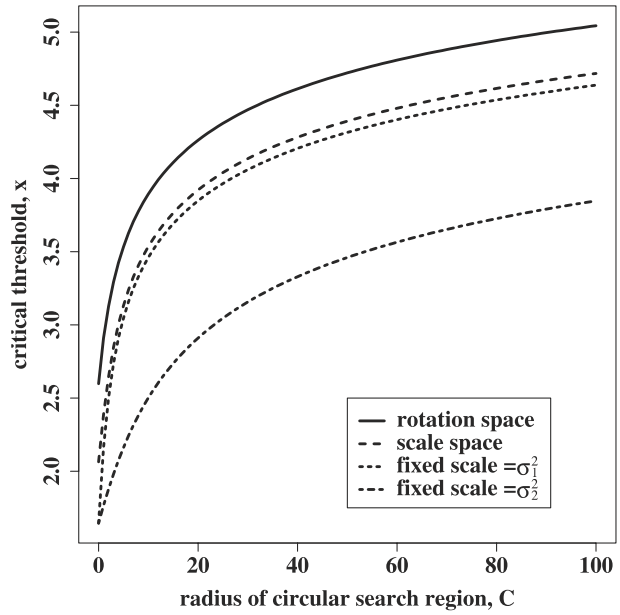

FIG. 5. *Comparison of critical values at the* 0.05 *level for a circular search region C with* $[\sigma_1^2, \sigma_2^2] = [2, 50]$, *as a function of the circle radius.*

4. The tubes approach. In this section, we study the same problem from the point of view of the volume of tubes, initiated in the classical papers of Hotelling (1939) and Weyl (1939) and developed for applications to statistics in Knowles and Siegmund (1989) and Naiman (1990), among others. Although neither the tube method nor the expected EC is guaranteed to be a good approximation to the probability of interest, in *geometrically well behaved problems* they seem to agree with each other [Siegmund and Worsley (1995) and Takemura and Kuriki (2002)] and to be reasonably accurate as judged by numerical comparisons with simulations. The present problem is *poorly behaved* in the sense that the rotation parameter is not identifiable when the scale parameters are equal. This manifests itself in a singularity in the five-dimensional space determined by two spatial, two scale and one rotation parameter, which induces local overlap in the tube. There is the additional, comparatively minor nuisance that the definition of the search space itself contains some arbitrariness not found in earlier related research.

We begin with the definition of the search space, for which we now propose to use $C \times Q^*$, where $Q^* = \{(l, m, \theta) : \sigma_1^2 \le m \le \sigma_2^2,\ c_1^2 m \le l \le c_2^2 m,\ 0 \le \theta \le \pi\}$ and $1 \le c_1 < c_2$. Since $\theta = \varphi/2$, some changes are only notational. Specifically, let $m = \sigma^2$ and $l/m = c^2$. Then $Q^* = \{(\theta, \sigma, c) : 0 \le \theta \le \pi,\ \sigma_1 \le \sigma \le \sigma_2,\ c_1 \le c \le c_2\}$. An important conceptual difference is that now the maximum value of the ratio, c_2, of the length of the major axis of the ellipse to the length of the minor axis

is the same for all permissible lengths of the minor axis (i.e., the ellipse is no longer required to become more circular when the minor axis approaches its maximum permitted length). Note that if $c_1 = 1$ and $c_2 = \sigma_2/\sigma_1$, then Q^* contains Q (see Figure 1). A second important difference is that by explicitly introducing the possibility that $c_1 > 1$, we are now providing a device to gather some information about the singular behavior that occurs at $c_1 = 1$. As a conceptual statistical matter, the first difference seems more important, but the mathematics connected with the second difference poses particularly challenging problems. Although this problem does not seem to pose a serious impediment to applications, we have not been able to solve it to our satisfaction. (See the remark at the end of this section.)

Note that if we replace the relations $1 \le c_1 < c_2$ by $c_1 < c_2 \le 1$, while leaving the constraints on l and m unchanged, or, equivalently, we interchange l and m while leaving c_1 and c_2 unchanged, we obtain a different search region. It would also be possible to consider the union of the two search regions, but we have not made the appropriate calculations.

We recall that the volume-of-tubes viewpoint is based first of all on the possibly fictitious assumption that the Gaussian field of interest, say $X(\mathbf{u})$, which is standardized to have mean function 0 and variance function 1 as $\mathbf{u}$ runs through an arbitrary indexing set, has a terminating Karhunen–Loève expansion, say $X(\mathbf{u}) = \sum_1^d \gamma_i(\mathbf{u}) Z_i$. Here the Z_i are independent standard normal random variables, and $\gamma(\mathbf{u}) = (\gamma_1(\mathbf{u}), \ldots, \gamma_d(\mathbf{u}))'$ is a vector of Euclidean norm equal to 1, which as a function of $\mathbf{u}$ defines a submanifold Γ of the unit sphere in d-dimensional Euclidean space. Since the final approximation depends only on quantities that can be calculated from the metric tensor of the manifold, the finiteness of d is not required for the approximating expression to make sense. Hence, we can and do use the tubes method whether the assumption of a finite expansion is satisfied or not. Little is known about the *mathematical* validity of the approximation when $d = \infty$ [see, however, Sun (1993)], but simulations show it is quite accurate. See Adler (2000) for a more thorough discussion.

Now we give the volume-of-tubes approximation when the kernel k can be expressed as $k(\mathbf{h}) = \pi^{-1/2} g(\mathbf{h}'\mathbf{h})$ for a one-dimensional nonincreasing function g defined on $[0, \infty)$ and satisfying $\int_0^\infty g(x)^2\, dx = 1$. The associated Gaussian field is defined by

$$X(\mathbf{t}, \mathbf{S}) = \pi^{-1/2} \det(\mathbf{S})^{-1/4} \int_{\mathbb{R}^2} g[(\mathbf{h} - \mathbf{t})' \mathbf{S}^{-1} (\mathbf{h} - \mathbf{t})]\, dW(\mathbf{h}),$$

where W is Gaussian white noise and $\mathbf{S}$ is a symmetric, positive-definite 2×2 matrix. With this notation, we can now state our approximation for the general radial kernel and $c_1 > 1$. The approximation for $c_2 < 1$ is obtained from (8) by changing the sign of the expression on the right-hand side of (8) and by changing the elliptic integral $E(\cdot)$ to $c^{-1} E[(1 - c^2)^{1/2}]$ each time it appears. For $c_1 = 1$, see below.

THEOREM 2. *For the rotation space random field with a general radial kernel, for each $\sigma_1 < \sigma_2$ and $1 < c_1 < c_2$, and as $x \to \infty$, we have*

$$
\begin{aligned}
&P\left\{\max_{(\mathbf{t},\theta,\sigma,c)\in C\times Q^*} X(\mathbf{t},\mathbf{S}) \ge x\right\} \\
&\quad\approx \frac{\phi(x)x^4}{(2\pi)^{5/2}}\frac{\pi\beta_1\beta_2(4\beta_2-1)^{1/2}|C|}{4}\frac{(1-r^2)}{\sigma_1^2}\left(2\log\frac{c_2}{c_1}+\frac{1}{c_2^2}-\frac{1}{c_1^2}\right) \\
&\qquad+\frac{\phi(x)x^3}{(2\pi)^2}\left\{\frac{\pi|C|\beta_1[\beta_2(6\beta_2-1)]^{1/2}}{4\sqrt{2}}\frac{(1+r^2)}{\sigma_1^2}\left(2\log\frac{c_2}{c_1}+\frac{1}{c_2^2}-\frac{1}{c_1^2}\right)\right. \\
&\qquad\qquad+\frac{\pi\beta_1[\beta_2(4\beta_2-1)]^{1/2}|C|}{2\sqrt{2}}\frac{(1-r^2)}{\sigma_1^2}\left(2-\frac{1}{c_2^2}-\frac{1}{c_1^2}\right) \\
&\qquad\qquad+\frac{\beta_2(\beta_1(4\beta_2-1))^{1/2}|\partial C|}{2^{1/2}}\frac{(1-r)}{\sigma_1} \\
&\qquad\qquad\qquad\left.\times\int_{c_1}^{c_2}\frac{c^2-1}{c^2}E\left[\left(\frac{c^2-1}{c^2}\right)^{1/2}\right]dc\right\} \\
&\qquad+\frac{\phi(x)x^2}{(2\pi)^{5/2}}\left\{\frac{\pi|C|\beta_1[-6\beta_2(4\beta_2-1)-(3\beta_2-1)]}{4(4\beta_2-1)^{1/2}}\right. \\
&\qquad\qquad\times\frac{(1-r^2)}{\sigma_1^2}\left(2\log\frac{c_2}{c_1}+\frac{1}{c_2^2}-\frac{1}{c_1^2}\right) \\
&\qquad\qquad-\beta_2(4\beta_2-1)^{1/2}\pi^2\chi(C)(\log r)\left(c_2-c_1+\frac{1}{c_2}-\frac{1}{c_1}\right) \\
&\qquad\qquad+\frac{(\beta_1\beta_2(6\beta_2-1))^{1/2}|\partial C|\pi}{2}\frac{(1+r)}{\sigma_1} \\
&\qquad\qquad\times\int_{c_1}^{c_2}\frac{c^2-1}{c^2}E\left[\left(\frac{c^2-1}{c^2}\right)^{1/2}\right]dc \\
&\qquad\qquad+\left(\beta_1\beta_2(4\beta_2-1)\right)^{1/2}|\partial C|\pi\frac{(1-r)}{\sigma_1} \\
&\qquad\qquad\times\sum_{i=1}^{2}\frac{c_i^2-1}{c_i}E\left[\left(\frac{c_i^2-1}{c_i^2}\right)^{1/2}\right] \\
&\qquad\qquad+\beta_1(2\beta_2)^{1/2}\pi|C|\frac{1}{\sigma_1^2} \\
&\qquad\qquad\times\left(\frac{c_1^2-1}{c_1^2}\left(r^2\arccos\beta_3+(\pi-\arccos\beta_3)\right)\right. \\
&\qquad\qquad\qquad\left.\left.+\frac{c_2^2-1}{c_2^2}\left(\arccos\beta_3+r^2(\pi-\arccos\beta_3)\right)\right)\right\},
\end{aligned}
\tag{7}
$$

where

$$\beta_1 = \int_0^\infty \dot{g}(x)^2 x\,dx, \qquad \beta_2 = \int_0^\infty \dot{g}(x)^2 x^2\,dx,$$
$$\beta_3 = [(4\beta_2 - 1)/(6\beta_2 - 1)]^{1/2}.$$

The formula for the Gaussian kernel $g(x) = \exp(-x/2)$ can be obtained by taking $\beta_1 = 1/4$ and $\beta_2 = 1/2$.

COROLLARY 1. *For the rotation space random field with a Gaussian kernel, we have*

$$\begin{aligned}
&P\left\{\max_{(\mathbf{t},\theta,\sigma,c)\in C\times Q^*} X(\mathbf{t},\theta,\sigma,c) \ge x\right\}\\
&\quad\approx \frac{\phi(x)x^4}{(2\pi)^{5/2}}\frac{\pi|C|}{32}\frac{(1-r^2)}{\sigma_1^2}\left(2\log\frac{c_2}{c_1}+\frac{1}{c_2^2}-\frac{1}{c_1^2}\right)\\
&\qquad+\frac{\phi(x)x^3}{(2\pi)^2}\left\{\frac{\pi|C|}{16\sqrt{2}}\frac{(1+r^2)}{\sigma_1^2}\left(2\log\frac{c_2}{c_1}+\frac{1}{c_2^2}-\frac{1}{c_1^2}\right)\right.\\
&\qquad\qquad+\frac{\pi|C|}{16}\frac{(1-r^2)}{\sigma_1^2}\left(2-\frac{1}{c_2^2}-\frac{1}{c_1^2}\right)\\
&\qquad\qquad\left.+\frac{|\partial C|}{4\sqrt{2}}\frac{(1-r)}{\sigma_1}\int_{c_1}^{c_2}\frac{c^2-1}{c^2}E\left[\left(\frac{c^2-1}{c^2}\right)^{1/2}\right]dc\right\}\\
&\qquad+\frac{\phi(x)x^2}{(2\pi)^{5/2}}\left\{\frac{(-7)\pi|C|}{32}\frac{(1-r^2)}{\sigma_1^2}\left(2\log\frac{c_2}{c_1}+\frac{1}{c_2^2}-\frac{1}{c_1^2}\right)\right.\\
&\qquad\qquad-\frac{\pi^2\chi(C)}{2}\log r\left(c_2-c_1+\frac{1}{c_2}-\frac{1}{c_1}\right)\\
&\qquad\qquad+\frac{|\partial C|\pi}{4}\frac{(1+r)}{\sigma_1}\int_{c_1}^{c_2}\frac{c^2-1}{c^2}E\left[\left(\frac{c^2-1}{c^2}\right)^{1/2}\right]dc\\
&\qquad\qquad+\frac{|\partial C|\pi}{2\sqrt{2}}\frac{(1-r)}{\sigma_1}\sum_{i=1}^{2}\frac{c_i^2-1}{c_i}E\left[\left(\frac{c_i^2-1}{c_i^2}\right)^{1/2}\right]\\
&\qquad\qquad\left.+\frac{\pi^2|C|}{16}\left(\frac{(c_1^2-1)}{c_1^2}\frac{(r^2+3)}{\sigma_1^2}+\frac{(c_2^2-1)}{c_2^2}\frac{(3r^2+1)}{\sigma_1^2}\right)\right\}.
\end{aligned}\tag{8}$$

This approximation involves the three leading terms in descending powers of x of the complete tube approximation, which, like the expected Hadwiger characteristic, contains five terms. For large x, these are the dominant terms, which involve the volume of the manifold Γ, the volume of its boundary $\partial\Gamma$, the scalar

curvature of the manifold and the geodesic mean curvature of the boundary [cf. Siegmund and Worsley (1995)]. If we rewrite (6) in decreasing powers of x up to three first leading terms, we have

$$
\begin{aligned}
&P\left\{\max_{(\mathbf{t},l,m,\varphi)\in C\times Q} X(\mathbf{t},l,m,\varphi)\geq x\right\}\\
&\quad\approx \frac{\phi(x)x^4}{(2\pi)^{5/2}}\frac{\pi|C|}{16\sigma_1^2}\{-(1+r^2)\log r-(1-r^2)\}\\
&\qquad+\frac{\phi(x)x^3}{(2\pi)^2}\left\{-\frac{\sqrt{2}\pi|C|}{16\sigma_1^2}(1-r^2)\log r\right.\\
&\qquad\qquad\left.+\frac{\sqrt{2}|\partial C|}{8\sigma_1}\int_0^{(1-r^2)^{1/2}}\left(\frac{t^3}{t'^3}-\frac{t^3 r}{t'^4}\right)E(t)\,dt\right\}\\
&\qquad+\frac{\phi(x)x^2}{(2\pi)^{5/2}}\left\{\frac{\pi|C|}{16\sigma_1^2}\{(2\pi+15)(1-r^2)+7(1+r^2)\log r\}\right.\\
&\qquad\qquad+\frac{\pi|\partial C|}{4\sigma_1}\int_0^{(1-r^2)^{1/2}}\left(\frac{t^3}{t'^3}-\frac{t^3 r}{t'^6}\right)E(t)\,dt\\
&\qquad\qquad\left.+\frac{\pi^{3/2}\chi(C)}{2}\left(2\log r-r+\frac{1}{r}\right)\right\}.
\end{aligned}
$$

We can see "corresponding" terms, which involve the same power of x, the same geometric characteristic of C and the same numerical constant, while expressions involving parameters of the search regions differ somewhat as a reflection of the differences in the definition of the search regions. As we indicate below, the approximation seems to be adequate for practical purposes. It would not, however, suffice to consider only the leading term. For the values of x that occur in typical examples, the second term is often larger than the first term, while the third term is comparatively small.

We have compared (8) with simulations in problems involving a small search space. The simulations are quite time consuming and would be difficult to carry out for a search space as large as those discussed above. The results indicate that (8) is reasonably accurate when $c_1 \geq 1.5$. [See Sigal (1998) for details.] The singular behavior of the rotation field at $c_1 = 1$ is such that in typical examples the approximation (8) begins to *decrease* as c_1 decreases from about 1.5, although the true probability must certainly increase. It is easy to explore numerically for the onset of this pathology and choose c_1 large enough to avoid it. This probably has negligible impact on the power. If it is thought desirable to include nearly spherical kernels in the search space, we recommend the following alternative approximation: set $c_1 = 1$ in (8) and add *twice* the leading term of the scale space P-value given in (4). This modified approximation has

the boundary term at c_1 deleted (since there is no boundary when $c_1 = 1$) and a term to account for the singularity at $c_1 = 1$ added. It results in a slightly more conservative P-value. For a numerical example, for C a circle of radius 50, $\sigma_1^2 = 2, \sigma_2^2 = 50$, $c_1 = 1.5$ and $c_2 = 5$, according to (8) the 0.05 significance level requires a threshold $x = 4.78$. (Note that this result is consistent with Figure 5.) For the same value of x and $c_1 = 1.25$, (8) gives 0.049; for $c_1 = 1$, it gives 0.044. Addition of the boundary correction suggested above puts the 0.05 threshold back up to $x = 4.80$ when $c_1 = 1$. Since the suggested alternative approximation is to some extent arbitrary, it is reassuring that the result does not depend critically on whether or not we use it.

For the fMRI example to be discussed in Section 6, but with the slightly larger search region used here, the 0.05 threshold obtained from (8) with $c_1 = 1.5$ is 4.59. The suggested modification at $c_1 = 1$ increases the threshold to 4.62.

REMARK. The fact that for c_1 close to 1 the formal tube volume can decrease as c_1 decreases is an indication of local overlap in the tube, which can lead to negative values for the Jacobian involved in the volume calculation. Siegmund and Zhang (1993) give a number of simple examples to show that the formal tube volume can badly underestimate the true volume, although that does not seem to occur here. To get some insight into this phenomenon in a very simple case, observe that if $\mathbf{t}$ and σ are held fixed in the metric tensor given in Appendix B, the surface defined by $\varphi = 2\theta$ and c behaves locally near $c = 1$ like the cone in three-dimensional space obtained by rotating the line $z = x$ in the xz-plane about the z-axis. The tube about this cone, considered as a surface in three-dimensional space, has local overlap in the interior of the cone near the vertex. It is straightforward to compute for a tube of (small) radius r the actual volume, the leading term of which is proportional to r times the square of the height of the cone. The true volume is larger than the formal Weyl volume by $\pi r^3/(3\sqrt{2})$, which is negligible when r is small compared to the height of the cone. The modified approximation suggested in the preceding paragraph is to some extent motivated by our analysis of this simple example.

5. Power. In this section, we will assume that a signal is actually present and that the shape of this signal is known, so that we can choose the kernel to match the signal, as in (2). Since we have assumed that the kernel is radially symmetric, we can write $k(\mathbf{h}) = \pi^{-1/2} g(\mathbf{h}'\mathbf{h})$ as in the previous section, where $g > 0$ is some decreasing and square integrable function of the squared radius. The matrix $\mathbf{S}_0^{-1}$ can be written as

$$\mathbf{S}_0^{-1} = \begin{bmatrix} \cos\theta_0 & -\sin\theta_0 \\ \sin\theta_0 & \cos\theta_0 \end{bmatrix} \begin{bmatrix} 1/\sigma_0^2 & 0 \\ 0 & 1/c_0^2\sigma_0^2 \end{bmatrix} \begin{bmatrix} \cos\theta_0 & \sin\theta_0 \\ -\sin\theta_0 & \cos\theta_0 \end{bmatrix},$$

so we obtain

$$dZ(\mathbf{t}) = \xi(\pi\sigma_0^2 c_0)^{-1/2} g[(\mathbf{t} - \mathbf{t}_0)'\mathbf{S}_0^{-1}(\mathbf{t} - \mathbf{t}_0)]\, d\mathbf{t} + dW(\mathbf{t}).$$

We are concerned with the probability

$$P\left\{\max_{\mathbf{u}\in C\times Q^*} X(\mathbf{u}) \geq x\right\},$$

where $X(\mathbf{u})$ is the convolution of $dZ(\mathbf{t})$ with the kernel k from some family parameterized by $\mathbf{u}$, which will be described below together with the set $C \times Q^*$ over which the maximization is taken. We will be interested primarily in two cases.

(i) The search is over rotation space, that is, $\mathbf{u} = (\mathbf{t}, \theta, \sigma, c)$,

$$X(\mathbf{t}, \theta, \sigma, c) = (\pi\sigma^2 c)^{-1/2} \int g[(\mathbf{h}-\mathbf{t})'\mathbf{S}^{-1}(\mathbf{h}-\mathbf{t})]\, dZ(\mathbf{h}).$$

It is also assumed that we search adaptively over $C \times Q^*$ (of the form discussed in the preceding section) containing the true values $\mathbf{t}_0, \sigma_0, c_0$ and $\theta \in [\theta_0 - \pi/2, \theta_0 + \pi/2]$.

(ii) The search is over scale space, that is, $\mathbf{u} = (\mathbf{t}, \sigma)$. This situation may arise, for example, if one would like to reduce computational effort or if it is assumed, possibly erroneously, that the signal is close to being isotropic.

For case (i), we obtain the power approximation

$$1 - \Phi(x-\xi) + \phi(x-\xi)\big(1 - (x/\xi)^{5/2}\big)/(\xi - x).$$

Since the calculations follow closely those of Siegmund and Worsley, we omit the details. Note that the calculations are based on simple expansions of the random field about the point in the search space where the signal is maximized, rather than the EC or tubes approaches of the previous sections.

For case (ii), the approximation is more complicated. The random field X is of the form

$$X(\mathbf{t}, \sigma) = \xi\mu(\mathbf{t}, \sigma) + (\pi\sigma^2)^{-1/2} \int g[(\mathbf{h}-\mathbf{t})'(\mathbf{h}-\mathbf{t})/\sigma^2]\, dW(\mathbf{h}),$$

where

$$\mu(\mathbf{t}, \sigma) = (\pi^2\sigma_0^2 c_0 \sigma^2)^{-1/2} \int g[(\mathbf{h}-\mathbf{t}_0)'\mathbf{S}_0^{-1}(\mathbf{h}-\mathbf{t}_0)] g[(\mathbf{h}-\mathbf{t})'(\mathbf{h}-\mathbf{t})/\sigma^2]\, d\mathbf{h}.$$

For the analysis of this case, we can assume that $\theta_0 = 0$. For the Gaussian kernel, it is easy to show that

$$\arg\left(\max_{(\mathbf{t},\sigma)\in C\times(0,\infty)} \mu(\mathbf{t}, \sigma)\right) = (\mathbf{t}_0, \sigma_0 c_0^{1/2}),$$

whenever C is a subset of $\mathbb{R}^2$ that contains the true location $\mathbf{t}_0$. In this case, $\mu(\mathbf{t}, \sigma)$ can be found in closed form as a convolution of two normalized two-dimensional Gaussian densities, which is again a normalized Gaussian density. For the general signal shape g, it can be shown through some manipulation of integrals

that $(\mathbf{t}_0, \sigma_0 c_0^{1/2})$ is a critical point of the function $\mu(\mathbf{t}, \sigma)$. The Gaussian kernel example gives a reason to believe that this is actually the point of global maximum for general g, although we have not succeeded in proving this rigorously. Let

$$\mu_0 = \mu(\mathbf{t}_0, \sigma_0 c_0^{1/2}) = \pi^{-1} \int g(\mathbf{h}'\mathbf{h}) g(\mathbf{h}'\mathbf{B}_0\mathbf{h})\, d\mathbf{h},$$

where $\mathbf{B}_0 = \begin{pmatrix} c_0 & 0 \\ 0 & 1/c_0 \end{pmatrix}$. In particular, for the Gaussian kernel $\mu_0 = 2c_0^{1/2}/(1 + c_0)$. If the scale space search region equals $C \times [\sigma_1, \sigma_2]$, where $[\sigma_1, \sigma_2]$ contains $\sigma_0 c_0^{1/2}$, then for the Gaussian kernels the final approximation takes the form

$$1 - \Phi(x - \xi\mu_0) + \phi(x - \xi\mu_0)(\xi\mu_0 - x)^{-1}(1 - \eta_1\eta_2),$$

where

$$\eta_1 = \left[(x^2(c_0 + 1)^2 - \xi^2\mu_0^2(c_0 - 1)^2)/(4\xi^2\mu_0^2 c_0)\right]^{1/2},$$
$$\eta_2 = \left[(x(c_0 + 1)^2 - \xi\mu_0(c_0 - 1)^2)/(4\xi\mu_0 c_0)\right]^{1/2}.$$

EXAMPLE. Assume that the signal can be well approximated by the elliptical Gaussian kernel with the smaller scale σ_0, which is believed to equal 1, but can be as small as 0.4 and as large as, say, 2.5. The ratio of axes c_0 is believed to be 2 but can be close to 1 (isotropic signal) or as large as 2.5. The signal can be located anywhere in $C = [-5, 5] \times [-5, 5]$ and is assumed to have unknown orientation. To test for the presence of such a signal, we use two methods. First, we search using elliptically shaped Gaussian kernels with $(\mathbf{t}, \theta, \sigma, c) \in C \times [0, \pi] \times [0.4, 2.5] \times [1, 2.5]$. Second, we search using spherical Gaussian kernels, with $(\mathbf{t}, \sigma) \in C \times [0.4, 2.5^{3/2}]$. We use the relative efficiency as the criterion to compare these two approaches. Assuming the amplitude ξ is proportional to the square root of the sample size, the efficiency is calculated as a square of the ratio of the amplitudes (call them ξ_e and ξ_s, where the subscripts e and s stand for elliptical and spherical correspondingly) necessary to achieve prespecified power. In particular, we will be interested in comparing the efficiency for different elongation parameters c_0. For rotation space, for the 5% threshold we obtained $x = 4.18$ from (8) with $c_1 = 1.5$, and $x = 4.23$ from (8) and (6) with $c_1 = 1$ (edge corrected). For our numerical examples, we have used the value $x_e = 4.18$. For scale space, we determined the threshold $x_s = 3.93$ from the equality (3.6) of Siegmund and Worsley (1995). Results for different values of the power β are presented in Table 1(a).

To allow for more elongated ellipses and a larger search region, we consider the same two tests but the corresponding regions are as follows:

1. $(\mathbf{t}, \theta, \sigma, c) \in [-100, 100] \times [-100, 100] \times [0, \pi] \times [0.4, 2.5] \times [2, 6]$;
2. $(\mathbf{t}, \sigma) \in [-100, 100] \times [-100, 100] \times [0.4\sqrt{2}, 2.5\sqrt{6}]$.

TABLE 1

Relative efficiency ξ_e^2/ξ_s^2 *of the two tests for* (a) *ellipses with ratio of axes close to* 1 *and* (b) *ellipses with ratio of axes moderately or significantly different from* 1. *The probability of detection of the signal is* β

(a)

	c_0	
β	**1.25**	**2.25**
0.85	0.99	0.89
0.90	1.00	0.89
0.95	1.00	0.89

(b)

	c_0	
β	**3.00**	**5.00**
0.85	0.87	0.69
0.90	0.87	0.69
0.95	0.87	0.69

This time, the threshold $x_e = 5.68$ is determined from the approximation (8), and $x_s = 5.17$. Results are presented in Table 1(b). As can be seen, for this choice of search region, our test is more efficient when the true ratio of axes is moderately or significantly different from 1.

6. Application. In this section, we shall apply the rotation space random field method to a simple fMRI experiment. One of the first experiments in fMRI was to locate the regions of the brain that respond to a simple visual stimulus [Kwong et al. (1992)]. In a similar experiment at the Montreal Neurological Institute, a subject was given a simple visual stimulus, flashing red dots, presented through light-tight goggles [Ouyang, Pike and Evans (1994)]. The stimulus was switched off for 4 scans, then on for 4 scans. This procedure was repeated 5 times, giving 40 scans. The time interval between scans was 6 seconds and the stimulus period was $T = 48$ seconds. Hence, the data consist of a time series of 40 two-dimensional images, each 128×128 pixels of size 2 mm. The response at one pixel is shown in Figure 6. Full details of the analysis can be found in Worsley (2001) where the data are analyzed using the χ^2 scale space method. To apply the rotation space method, we fit a linear model at each pixel in sine and cosine waves with a period matching that of the stimulus. The coefficients of these two components, normalized to have unit variance, are shown in Figure 7. These images will be referred to as sine and cosine components of the data. The phase was chosen so that we expect all the signal to be in the cosine component (shown in Figure 6 at one pixel), whereas the sine component should have no signal (zero mean). The rotation space method was applied to both components separately. Based on previous analyses, the search region for l and m, $[\sigma_1^2, \sigma_2^2]$, was chosen to be $[2.55^2, 12.75^2]$ so that $r = \sigma_1/\sigma_2 = 0.2$.

The global maximum of the sine component is 3.69 at location $(t_1, t_2) = (168, 54)$ mm and filter $\mathbf{s} = (12.75^2, 12.75^2, 0°)$. For the cosine component, the global maximum is 14.87 at location $(t_1, t_2) = (138, 68)$ mm and filter $\mathbf{s} = (5.70^2, 2.55^2, 144°)$. The images of the sine and cosine components smoothed with

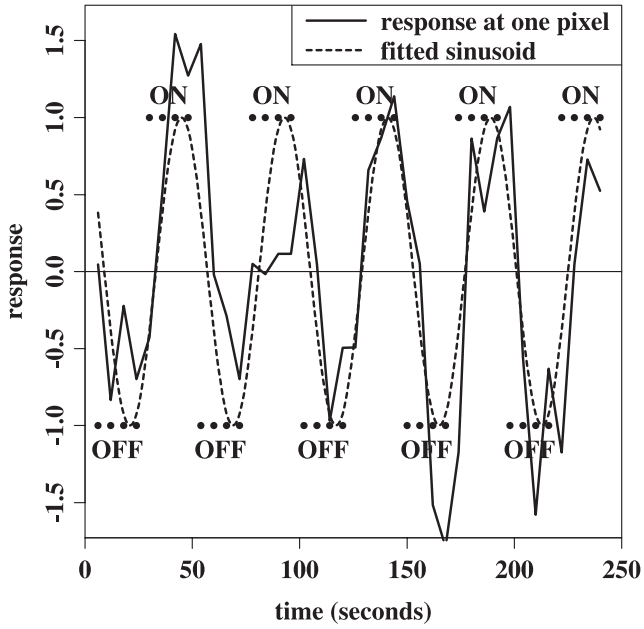

FIG. 6. *ON–OFF stimulus, response at one pixel and fitted sinusoid for the fMRI data.*

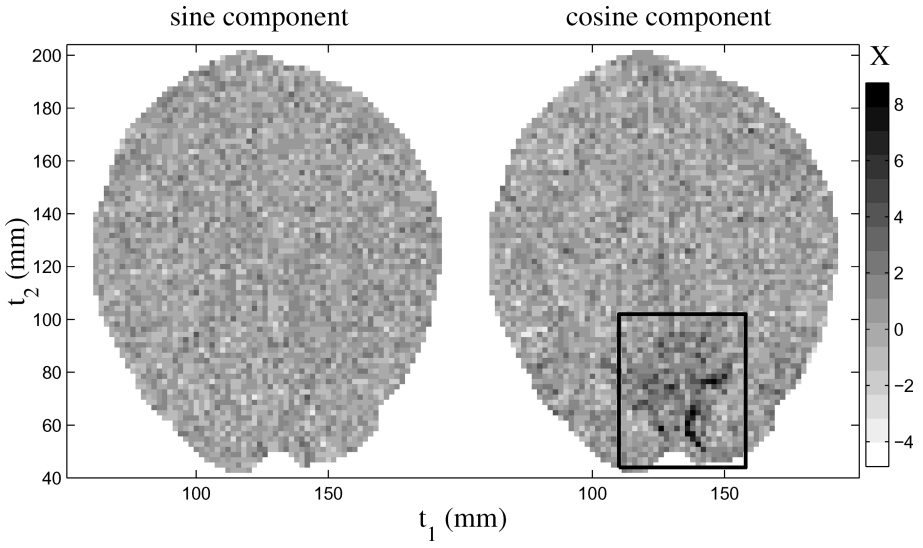

FIG. 7. *Sine and cosine components of the fMRI data. See Figure* 10 *for a detail of the boxed region.*

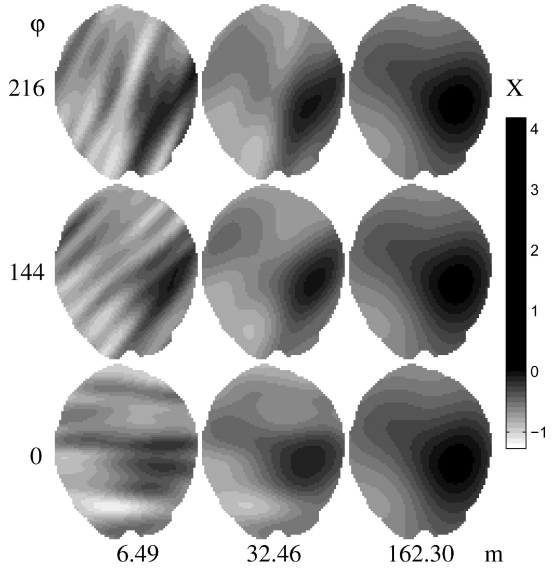

FIG. 8. *Sine component smoothed with different values of m and φ. The value of l is fixed at* 162.30. *The lower right image is the smoothed image with the maximizing filter.*

some values of **s**, including the maximizing ones, are shown in Figures 8 and 9, respectively.

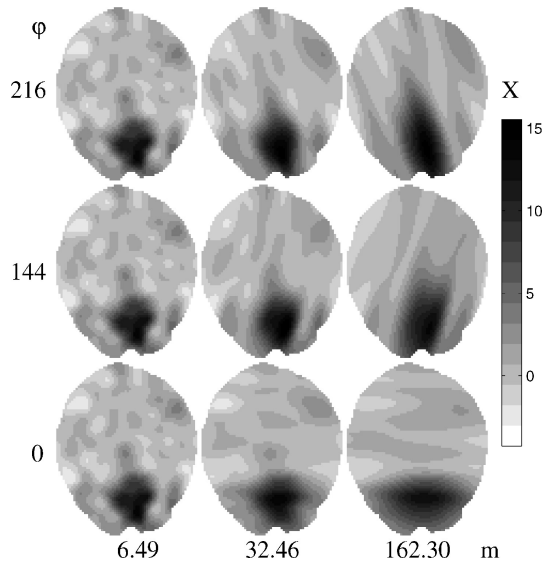

FIG. 9. *Cosine component smoothed with different values of l and φ. The value of m is fixed at* 6.49. *The middle image is the smoothed image with the maximizing filter.*

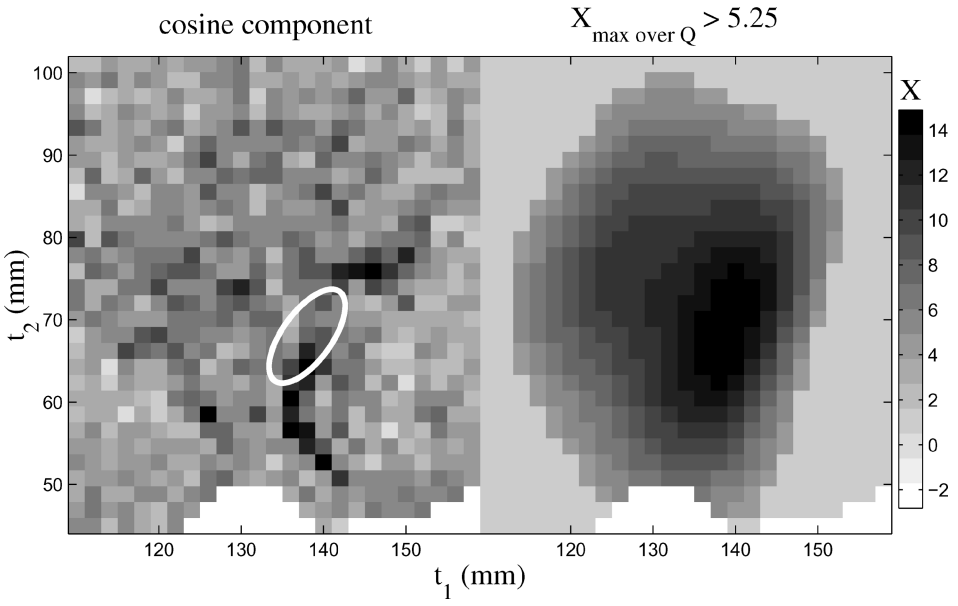

FIG. 10. *Left*: *detail of the cosine component* (*outlined in Figure* 7) *along with a contour of the maximizing filter at half its height*, *outlined in white*. *Right*: *the same detail but showing the maximum of X over all scales and rotations*, $\max_{\mathbf{s}\in Q} X(\mathbf{t}, \mathbf{s})$, *thresholded at the* $p = 0.05$ *critical value of* 5.25, *which covers most of the visual cortex*.

For the purpose of finding the P-value, the slice of the brain was approximated by a circle of radius 61.77 mm chosen so that its area matched that of the slice. Hence, $|C| = 11{,}960$ mm^2, $|\partial C| = 388$ mm and $\chi(C) = 1$. Then $\mathrm{E}[\chi(A_x)]$ was calculated using (6). To find the critical value, this expectation was equated to 0.05 and solved for the value of x. The critical value at the level of 0.05 was found to be 4.52. Therefore, the result for the maximum of the sine component is not significant, but the result for the cosine component is highly significant. The images of the cosine component, along with a contour of the maximizing filter, and the excursion set for the location above the critical value of 0.05 are shown in Figure 10. This indicates that the activation was taking place in the visual cortex as expected.

7. Conclusion. In this paper, we obtained the expected EC for the Gaussian rotation space random field with a Gaussian kernel when $N = 2$. This result can be used as an approximation of the null distribution of the test statistic $X_{\max}$ for detecting ellipsoidal-shaped signals. A feature of the derivation is the use of MAPLE to perform extensive algebraic manipulations. Using the MAPLE code in the Appendix of Shafie (1998) (available at www.math.mcgill.ca/shafie), one can extend the result to more general smoothing kernels. The calculation of the expected EC can also be extended to the χ^2 rotation space random field.

We have also used the volume-of-tubes method to derive a three-term approximation to the distribution of $X_{\max}$ and have shown that this approach gives essentially the same numerical results as those based on the expected EC.

The method proposed in this paper for detecting signals in a noisy image has the potential advantage of greater sensitivity at detecting signals of rotated elliptical shapes. The disadvantage of this method is that signals which are close together might be detected as a single broader signal rather than separate signals. Another limitation of the method is the time required to search for the global maximum over the five-dimensional rotation space (although this is less an impediment to data analysis, where the search must only be done once, than to an evaluation of the P-value by simulation, where the search must be done repeatedly).

In a brief power comparison, we have shown that the rotation space field is moderately more efficient than the scale space field when the true signal has an elliptical shape.

The theory developed and the images analyzed in the paper are two-dimensional. Most often, the images of the brain are collected in three-dimensional space. In principle, the method can be applied to three dimensions, but now the search space is nine-dimensional (three for location, six for rotation and scaling) which would enormously complicate both the theory and the application.

A potential area of application that we have not explored is the detection of line segments or broken lines representing, for example, faults in materials or edges of images.

APPENDIX A

Proof of Theorem 1. Before going through the proof of Theorem 1, note that in the following the joint distribution of X and a subvector X_a of $\dot{\mathbf{X}}$ is denoted by ϕ_a. Also, symmetric submatrices of $\ddot{\mathbf{X}}$ are treated interchangeably as a matrix or a vector. The vector version of these submatrices, derived as explained above, is used for distributional purposes. For simplicity, we will denote $\dot{X}_a$ ($\dot{X}_a > 0$) and $\dot{X}_a$ ($\dot{X}_a < 0$) by $\dot{X}_a^+$ and $\dot{X}_a^-$, respectively. Also, we denote the contribution of the set $B \cap A_x$ to the EC of excursion set A_x by $\mathrm{Con}(B)$.

A.1. *Contribution of* $C^\circ \times Q^\circ$. The contribution of $C^\circ \times Q^\circ$ is similar to the contribution of the interior of the prism in (3). Let φ be the last coordinate, so that from (3) we have

$$\mathrm{Con}(C^\circ \times Q^\circ) = \int_{C\times Q} \mathrm{E}[\dot{X}_\varphi^+ \det(-\ddot{\mathbf{X}}_{12lm}) | X = x, \dot{\mathbf{X}}_{12lm} = \mathbf{0}]\phi_{12lm}(x, \mathbf{0})\, d\mathbf{s}\, d\mathbf{t}.$$

To calculate the expectation in the integrand of $\mathrm{Con}(C^\circ \times Q^\circ)$, we first condition

on $\dot{X}_\varphi$. The distribution of $\ddot{\mathbf{X}}_{12lm}$ given $(X = x, \dot{\mathbf{X}}_{12lm} = \mathbf{0}, \dot{X}_\varphi)$ is $N(\boldsymbol{\mu}, \Sigma)$ with

$$\boldsymbol{\mu} = \frac{1}{8}\Bigg[-2\frac{(l+m-(l-m)\cos(\varphi))x}{lm} - 16\frac{\sin(\varphi)\dot{X}_\varphi}{l-m},$$
$$2\frac{\sin(\varphi)(l-m)x}{lm} + 16\frac{\cos(\varphi)\dot{X}_\varphi}{l-m}, 0, 0,$$
$$-2\frac{(l+m+(l-m)\cos(\varphi))x}{lm} + 16\frac{\sin(\varphi)\dot{X}_\varphi}{l-m}, 0, 0, -\frac{x}{l^2}, 0, -\frac{x}{m^2}\Bigg]',$$

and $\Sigma = [V_1, V_2, V_3]$. The matrices V_1, V_2 and V_3 are given in the Appendix of Shafie (1998).

Using MAPLE, we get

$$\mathrm{E}[\det(-\ddot{\mathbf{X}}_{12lm}) | X = x, \dot{\mathbf{X}}_{12lm} = \mathbf{0}, \dot{X}_\varphi]$$
$$= -\frac{(x^2-1)\dot{X}_\varphi^2}{16(l-m)^2 l^2 m^2} + \frac{10 + x^4 - 9x^2}{256 m^3 l^3}.$$

The random variable $\dot{X}_\varphi$ is independent of $(X, \dot{\mathbf{X}}_{12lm})$ and is distributed as $N(0, (l-m)^2/16lm)$. The joint density of $(X, \dot{\mathbf{X}}_{12lm})$ evaluated at $(x, \mathbf{0})$ is

$$\phi_{12lm}(x, \mathbf{0}) = \frac{(lm)^{3/2}}{16(2\pi)^{5/2}} e^{-x^2/2}.$$

Since

$$\mathrm{E}[\dot{X}_\varphi^j (\dot{X}_\varphi > 0)] = \mathrm{Var}(\dot{X}_\varphi)^{j/2} 2^{(j-1)/2} \Gamma[(j+1)/2]/(2\pi)^{1/2},$$

we get

$$\mathrm{E}[\dot{X}_\varphi^+ \det(-\ddot{\mathbf{X}}_{12lm}) | X = x, \dot{\mathbf{X}}_{12lm} = \mathbf{0}] \phi_{12lm}(x, \mathbf{0}) = \frac{(l-m)}{512\pi^3 m^2 l^2} h(x),$$

where $h(x) = (x^4 - 11x^2 + 12)e^{-x^2/2}$. After integration on Q and C, we obtain

$$\mathrm{Con}(C^\circ \times Q^\circ)$$
$$= \frac{|C|}{256\pi^2}\left(\frac{\log\sigma_2^2}{\sigma_2^2} - \frac{\log\sigma_1^2}{\sigma_2^2} + \frac{2}{\sigma_2^2} - \frac{2}{\sigma_1^2} + \frac{\log\sigma_2^2}{\sigma_1^2} - \frac{\log\sigma_1^2}{\sigma_1^2}\right) h(x).$$

A.2. *Contribution of $\partial C \times Q^\circ$ to the expected EC.* The set $\partial C \times Q^\circ$ is a part of the boundary of the search region, so to obtain its contribution we use the form for boundaries as in (3). Since Q is flat in the topological sense, the gradient vector in the tangent plane to $\partial C \times Q^\circ$ has the form of $\dot{\mathbf{X}}_{\mathrm{T}lm}$ and the Hessian matrix in the tangent plane is equal to $\ddot{\mathbf{X}}_{\mathrm{T}lm}$, where the subscript T shows derivative in the direction of the tangent to ∂C. Also, the normal to $\partial C \times Q^\circ$ at a point $(\mathbf{t}, l, m, \varphi), \mathbf{t} \in \partial C$, is parallel to the normal to ∂C at the point $\mathbf{t}$, thus,

$X_\perp$ is the derivative of X in the direction of the inside normal to ∂C. By the same reasoning (flatness of Q), the curvature matrix of $\partial C \times Q^\circ$ has the form

$$\mathbf{c} = \begin{pmatrix} c & 0 & 0 \\ 0 & 0 & 0 \\ 0 & 0 & 0 \end{pmatrix},$$

where c is the scalar curvature of ∂C. Therefore,

$$\begin{aligned}\mathrm{Con}(\partial C \times Q^\circ) = \int_{\partial C} \int_{\mathbf{s}} \mathrm{E}[\dot{X}_\varphi^+ \det(-\ddot{\mathbf{X}}_{\mathrm{T}lm} - \dot{X}_\perp \mathbf{c})(\dot{X}_\perp < 0) | X = x, \dot{\mathbf{X}}_{\mathrm{T}lm} = \mathbf{0}] \\ \times \phi_{\mathrm{T}lm}(x, \mathbf{0})\, d\mathbf{s}\, d\mathbf{t}_{\mathrm{T}}.\end{aligned}$$

At each fixed point on ∂C, denote the coordinates of a point with respect to the unit tangential and normal vectors by (u_1, u_2). The change of coordinates from (u_1, u_2) to (t_1, t_2) is done by a rotation matrix. After taking the expectation in the above equation, we are integrating over all possible rotations; hence, without loss of generality, we can replace $\ddot{\mathbf{X}}_{\mathrm{T}lm}$ by $\ddot{\mathbf{X}}_{1lm}$ and $\dot{X}_\perp$ by $\dot{X}_2$.

After these substitutions, by expanding the determinant, the expectation in the integrand can be written as

$$\begin{aligned}&\mathrm{E}[\dot{X}_\varphi^+ \det(-\ddot{\mathbf{X}}_{1lm} - \dot{X}_2 \mathbf{c})(\dot{X}_2 < 0) | X = x, \dot{\mathbf{X}}_{1lm} = \mathbf{0}] \\ &\quad = \mathrm{E}[\dot{X}_\varphi^+ \det(-\ddot{\mathbf{X}}_{1lm})(\dot{X}_2 < 0) | X = x, \dot{\mathbf{X}}_{1lm} = \mathbf{0}] \\ &\qquad - c\mathrm{E}[\dot{X}_\varphi^+ \det(\ddot{\mathbf{X}}_{lm}) \dot{X}_2 (\dot{X}_2 < 0) | X = x, \dot{\mathbf{X}}_{1lm} = \mathbf{0}].\end{aligned}$$

Hence, we can write

$$\mathrm{Con}(\partial C \times Q^\circ) = \mathrm{Con}(\partial C \times Q^\circ)_1 + \mathrm{Con}(\partial C \times Q^\circ)_2,$$

where

$$\begin{aligned}&\mathrm{Con}(\partial C \times Q^\circ)_1 \\ &\quad = \int_{\partial C} \int_Q \mathrm{E}[\dot{X}_\varphi^+ \det(-\ddot{\mathbf{X}}_{1lm})(\dot{X}_2 < 0) | X = x, \dot{\mathbf{X}}_{1lm} = \mathbf{0}] \phi_{1lm}(x, \mathbf{0})\, d\mathbf{t}_{\mathrm{T}}\, d\mathbf{s}\end{aligned}$$

and

$$\begin{aligned}&\mathrm{Con}(\partial C \times Q^\circ)_2 \\ &\quad = -\int_{\partial C} \int_Q c\mathrm{E}[\dot{X}_\varphi^+ \det(\ddot{\mathbf{X}}_{lm}) \dot{X}_2 (\dot{X}_2 < 0) | X = x, \dot{\mathbf{X}}_{1lm} = \mathbf{0}] \phi_{1lm}(x, \mathbf{0})\, d\mathbf{t}_{\mathrm{T}}\, d\mathbf{s}.\end{aligned}$$

For the first part, we have

$$\begin{aligned}&\mathrm{E}[\dot{X}_\varphi^+ \det(-\ddot{\mathbf{X}}_{1lm})(\dot{X}_2 < 0) | X = x, \dot{\mathbf{X}}_{1lm} = \mathbf{0}] \phi_{1lm}(x, \mathbf{0}) \\ &\quad = -\left(\frac{\sqrt{2} x (l - m) \sin(\varphi)^2 \sigma_2^3}{256 \pi^{5/2} m l} - \frac{\sqrt{2}(l^2 - m^2)(x^3 - 5x)\sigma_2}{1024 \pi^{5/2} m^2 l^2} \right) e^{-x^2/2} \\ &\qquad - \left(\frac{\sqrt{2}(l - m)^2 (x^3 - 5x)}{1024 \pi^{5/2} m^2 l^2} \cos(\varphi) - \frac{(l - m)(x^2 - 1)}{512 l^{3/2} \pi^2 m^{3/2}} \sin(\varphi) \right) \sigma_2 e^{-x^2/2},\end{aligned}$$

where $\sigma_2^2 = 1/((l+m-(l-m)\cos(\varphi))$ is the conditional variance of $\dot{X}_2$ given $\dot{X}_1$. Integrating over φ and m, we have

$$\mathrm{Con}(\partial C \times Q^\circ)_1 = |\partial C| \int_0^{\sqrt{1-r^2}} f_1(t)\,dt,$$

where

$$f_1(t) = \frac{e^{-x^2/2}}{32\pi^{5/2}\sigma_1} \frac{(\sqrt{1-t^2}-r)}{(1-t^2)^2 t} \big[\big((x^3-5x)t^4 - 8xt^2 + 8x\big)E(t) + (-4xt^4 + 12xt^2 - 8x)K(t)\big].$$

Using the Gauss–Bonnet theorem $\int_{\partial C} c\,d\mathbf{t}_{\mathrm{T}} = 2\pi\chi(C)$, for the second part we have

$$\begin{aligned}\mathrm{Con}(\partial C \times Q^\circ)_2 &= -\frac{\chi(C)}{64}(x^2-1)e^{-x^2/2} \int_{\sigma_1^2}^{\sigma_2^2} \int_{\sigma_1^2}^{l} \int_0^{2\pi} \frac{(l-m){\sigma_2}^2}{\pi^2 lm}\,d\varphi\,dm\,dl \\ &= \frac{\chi(C)}{16\pi}\left(2\log r - r + \frac{1}{r}\right)(x^2-1)e^{-x^2/2}.\end{aligned}$$

A.3. *Contribution of $C^\circ \times \partial Q$ to the expected EC.* To obtain $\mathrm{Con}(C^\circ \times \partial Q)$, we use the partition (5) of ∂Q. Since the rotation random field X is the same on B_3 and B_4, these two sets have no contribution to the EC of the excursion set. So we will obtain the contribution of the other parts of ∂Q, starting with $\mathrm{Con}(C^\circ \times B_1)$.

A.3.1. $\mathrm{Con}(C^\circ \times B_1)$. Since the set $C^\circ \times B_1$ is flat, the curvature matrix is 0. The inward normal to this set is in the direction of m. Hence, we have

$$\begin{aligned}&\mathrm{Con}(C^\circ \times B_1) \\ &\quad = \int_C \int_0^{2\pi} \int_{\sigma_1^2}^{\sigma_2^2} \mathrm{E}[\dot{X}_\varphi^+ \det(-\ddot{\mathbf{X}}_{12l})(\dot{X}_m < 0) | X = x, \dot{\mathbf{X}}_{12l} = \mathbf{0}] \\ &\qquad\qquad \times \phi_{12l}(x, \mathbf{0})\,dl\,d\varphi\,d\mathbf{t}.\end{aligned}$$

Evaluating the expectation in the integrand, we get

$$\begin{aligned}&\mathrm{E}[\dot{X}_\varphi^+ \det(-\ddot{\mathbf{X}}_{12\,l})(\dot{X}_m < 0) | X = x, \dot{\mathbf{X}}_{12l} = \mathbf{0}]\phi_{12l}(x, \mathbf{0}) \\ &\quad = -\frac{(6 - 2x^2 + 6\sqrt{\pi}x - \sqrt{\pi}x^3)(l - \sigma_1^2)e^{-x^2/2}}{256\pi^3\,\sigma_1^2 l^2}.\end{aligned}$$

Integrating with respect to l, φ and $\mathbf{t}$ and substituting $m = \sigma_1^2$, we obtain

$$\begin{aligned}&\mathrm{Con}(C^\circ \times B_1) \\ &\quad = \frac{|C|}{128\pi^2}\left[\frac{-2\log r - 1}{\sigma_1^2} + \frac{r^2}{\sigma_1^2}\right](x^3\sqrt{\pi} + 2x^2 - 6x\sqrt{\pi} - 6)e^{-x^2/2}.\end{aligned}$$

A.3.2. $\mathrm{Con}(C^\circ \times B_2)$. The set $C^\circ \times B_2$ is also flat. So the curvature matrix is 0, but the inward normal to this set is in the opposite direction of l. Therefore,

$$\begin{aligned}&\mathrm{Con}(C^\circ \times B_2)\\ &\quad= \int_C \int_0^{2\pi} \int_{\sigma_1^2}^{\sigma_2^2} \mathrm{E}[\dot{X}_\varphi^+ \det(-\ddot{\mathbf{X}}_{12m})(\dot{X}_l > 0) | X = x, \dot{\mathbf{X}}_{12m} = \mathbf{0}]\\ &\qquad\qquad \times \phi_{12m}(x, \mathbf{0})\, dm\, d\varphi\, d\mathbf{t}.\end{aligned}$$

By the same procedure as in the previous section, we get

$$\begin{aligned}&\mathrm{Con}(C^\circ \times B_2)\\ &\quad= -\frac{|C|}{128\pi^2}\left[\frac{-2\log r + 1}{\sigma_2^2} - \frac{1}{\sigma_1^2}\right](x^3\sqrt{\pi} - 2x^2 - 6x\sqrt{\pi} + 6)e^{-x^2/2}.\end{aligned}$$

A.3.3. $\mathrm{Con}(C^\circ \times L)$. The set $C^\circ \times L$ has a different nature from $C^\circ \times B_1$ and $C^\circ \times B_2$. Although the set is flat so that the curvature matrix is 0, there is no unique normal to this set. To make sure the derivative in the direction of the inside normal is negative, we have to consider all the directions from the m-axis to the l-axis. To do this, it is enough to make sure that the derivative in the direction of l is positive and the derivative in the direction of m is negative. Therefore, the contribution of $C^\circ \times L$ will be

$$\begin{aligned}&\mathrm{Con}(C^\circ \times L)\\ &\quad= \int_C \int_0^{2\pi} \mathrm{E}[\dot{X}_\varphi^+ \det(-\ddot{\mathbf{X}}_{12})(\dot{X}_l > 0)(\dot{X}_m < 0) | X = x, \dot{\mathbf{X}}_{12} = \mathbf{0}]\\ &\qquad\qquad \times \phi_{12}(x, \mathbf{0})\, d\varphi\, d\mathbf{t}.\end{aligned}$$

Evaluation of the expectation in the integrand gives us

$$\begin{aligned}&\mathrm{E}[\dot{X}_\varphi^+ \det(-\ddot{\mathbf{X}}_{12})(\dot{X}_l > 0)(\dot{X}_m < 0) | X = x, \dot{\mathbf{X}}_{12} = \mathbf{0}]\phi_{12}(x, \mathbf{0})\\ &\quad= \frac{(\pi x^2 - 2\pi - 4)(\sigma_2^2 - \sigma_1^2)e^{-x^2/2}}{128\sigma_1^2\sigma_2^2\pi^3}.\end{aligned}$$

Integration with respect to φ and $\mathbf{t}$ gives the result

$$\mathrm{Con}(C^\circ \times L) = \frac{(-2\pi + \pi x^2 - 4)(\sigma_2^2 - \sigma_1^2)e^{-x^2/2}}{64\pi^2\sigma_1^2\sigma_2^2}.$$

A.4. *Contribution of $\partial C \times \partial Q$ to the expected EC.* We now obtain the contribution of $\partial C \times \partial Q$, again partitioning ∂Q as in (5). The sets B_3 and B_4 again have no contribution. For the other parts, B_1, B_2 and L, the same argument

as in Sections A.2 and A.3 applies to get

$$\mathrm{Con}(\partial C \times B_1) = |\partial C| \int_0^{\sqrt{1-r^2}} f_2(t)\,dt + \frac{\chi(C)}{16\sqrt{\pi}}\left[r + \frac{1}{r} - 2\right] x e^{-x^2/2},$$

$$\mathrm{Con}(\partial C \times B_2) = |\partial C| \int_0^{\sqrt{1-r^2}} f_3(t)\,dt + \frac{\chi(C)}{16\sqrt{\pi}}\left[r + \frac{1}{r} - 2\right] x e^{-x^2/2},$$

$$\mathrm{Con}(\partial C \times L) = |\partial C| f_4 - \chi(C)\frac{(\sigma_2^2 - \sigma_1^2)e^{-x^2/2}}{16\sigma_1\sigma_2},$$

where

$$f_2(t) = \frac{e^{-x^2/2}}{32\pi^{5/2}\sigma_1}\frac{1}{t(1-t^2)^{3/2}}\big[\big(\sqrt{\pi}(x^2-3)t^4 - 2(\sqrt{\pi}-x)t^2 + 4\sqrt{\pi}\big)E(t) + \big(2xt^4 + (4\sqrt{\pi}-2x)t^2 - 4\sqrt{\pi}\big)K(t)\big],$$

$$f_3(t) = \frac{e^{-x^2/2}}{32\pi^{5/2}\sigma_2^2}\frac{1}{t(1-t^2)^3}\big[\big((\sqrt{\pi}x^2 - \sqrt{\pi} + 2x)t^4 + (-2x - 6\sqrt{\pi})t^2 + 4\sqrt{\pi}\big)E(t) + \big((2x - 4\sqrt{\pi})t^4 + (8\sqrt{\pi} - 2x)t^2 - 4\sqrt{\pi}\big)K(t)\big].$$

A.5. *Contribution of $C \times P$ to the expected EC.* In P, we have $l = m$, in which case, as we discussed before, φ disappears and the rotation space random field reduces to the scale space random field. To obtain $\mathrm{Con}(C \times P)$, we can use (4) for the Gaussian kernel case. For the Gaussian kernel, $\kappa = 1$, $\beta = 1/2$. By substituting these values and $N = 2$ in (4), we have

$$\begin{aligned}\mathrm{Con}(C \times P) &= |C|\sigma_1^{-2}/2\big\{(2\pi)^{-1/2}(1-r^2)x^2/2 + (1+r^2)x/2\big\}\phi(x)/(2\pi)\\ &\quad + |\partial C|2^{-1/2}\sigma_1^{-1}\big\{(2\pi)^{-1/2}(1-r)x/2 + (1+r)/4\big\}\phi(x)/(2\pi)^{1/2}\\ &\quad + \chi(C)\big\{-(2\pi)^{-1/2}\log r\,\phi(x) + [1-\Phi(x)]\big\}.\end{aligned}$$

APPENDIX B

Tube derivations. Here we assume that X is as defined in Section 2 with the Gaussian kernel given in (1). Similar calculations apply to a general radial kernel. It will be convenient to put $\mathbf{S}^{-1} = \mathbf{A}$, with entries (a_{ij}). We initiate derivation of (8) by considering the volume of a tube of geodesic radius ϕ around the five-dimensional manifold $\Gamma = \{\gamma(\mathbf{t}, \theta, \sigma, c) : (\mathbf{t}, \theta, \sigma, c) \in C \times Q^*;\ Q^* = [0, \pi] \times [\sigma_1, \sigma_2] \times [c_1, c_2],\ c_1 > 1\}$ embedded in the unit sphere S^{d-1} in $\mathbb{R}^d$.

The metric tensor of the manifold is the basis for all calculations. The elements $[g_{ij}]_{i,j=1}^5$ of the metric tensor g can be expressed through the partial derivatives of

the covariance function R of the random field as follows: putting $\mathbf{u} = (\mathbf{t}, \theta, \sigma, c)$, we have

$$g_{ij}(\mathbf{u}) = \sum_{k=1}^{d} \frac{\partial \gamma_k(\mathbf{u})}{\partial u_i} \frac{\partial \gamma_k(\mathbf{u})}{\partial u_j} = \frac{\partial^2 R(\mathbf{u}_1; \mathbf{u}_2)}{\partial u_i \partial u_j}\bigg|_{\mathbf{u}_1 = \mathbf{u}_2}.$$

The result of substantial calculation [cf. Sigal (1998)] is the metric tensor

$$g = \begin{bmatrix} a_{11}/2 & a_{12}/2 & 0 & 0 & 0 \\ a_{12}/2 & a_{22}/2 & 0 & 0 & 0 \\ 0 & 0 & (c^2-1)^2/(4c^2) & 0 & 0 \\ 0 & 0 & 0 & 1/\sigma^2 & 1/(2\sigma c) \\ 0 & 0 & 0 & 1/(2\sigma c) & 1/(2c^2) \end{bmatrix}.$$

To find the volume of a tube, we split the calculations into pieces corresponding to the different parts of the tube.

We start by considering the points z inside the tube that are closest (in the sense of a distance in Euclidean space $\mathbb{R}^d$) to a point γ in the interior of the manifold Γ. We use the notation $T_{\Gamma^o}(\phi)$ for this part of the tube. At each point of the manifold, the five-dimensional tangent space is spanned by the vectors $(\gamma_{t_1}, \gamma_{t_2}, \gamma_\theta, \gamma_\sigma, \gamma_c)$. Let $n(0), n(1), \ldots, n(d-6)$ be the $d-5$ orthonormal vectors, normal to the tangent space of Γ and lying in the tangent space of S^{d-1} for $i = 1, \ldots, d-6$, $n(0) = \gamma(\mathbf{t}, \theta, \sigma, c)$. For notational convenience, we will occasionally use $\mathbf{u} = (u_1, u_2, u_3, u_4, u_5)$ to denote the quintuple $(\mathbf{t}, \theta, \sigma, c)$. Then z can be represented as $z = y/\|y\|$, where

$$y = y(\mathbf{u}, \xi_1, \ldots, \xi_{d-6}) = \gamma + \xi_1 n(1) + \cdots + \xi_{d-6} n(d-6),$$

$\|y\| = (1 + \sum_{i=1}^{d-6} \xi_i^2)^{1/2}$, $\sum_{i=1}^{d-6} \xi_i^2 \le \tan^2 \phi$. Also [see, e.g., Lemma 1 of Knowles and Siegmund (1989)], we have

$$dV_{\Gamma^o}(z) = \|y, y_1, \ldots, y_5, n(1), \ldots, n(d-6)\| \frac{d\mathbf{u}\, d\xi_1 \cdots d\xi_{d-6}}{(1 + \sum_{i=1}^{d-6} \xi_i^2)^{d/2}},$$

where y_i, $i = 1, \ldots, 5$, denotes the partial derivative of y with respect to u_i and $\|\cdot\|$ denotes the absolute value of the determinant. According to Weyl (1939), the part of the volume $V_\Gamma(\phi)$ arising from this part of the tube is

$$\begin{aligned} V_{\Gamma^o}(\phi) &= (\le)\, \omega_{m-1} \sum \kappa_e J_e(\phi) \\ &= \omega_{m-1}\big(\kappa_0 J_0(\phi) + \kappa_2 J_2(\phi)\big) + o\big(J_2(\phi)\big), \qquad \phi \to 0, \end{aligned} \tag{9}$$

e even, $0 \le e \le 5$, $m = d-6$. Here ω_{m-1} is a surface area of the unit sphere S^{m-1}, κ_e equals certain integrals with respect to the volume element of the manifold Γ

and $J_e(\phi)$ is an incomplete beta function

$$J_0(\phi) = \int_0^\phi (\sin\omega)^{m-1}(\cos\omega)^n \, d\omega,$$

$$m(m+2)\cdots(m+e-2)J_e(\phi) = \int_0^\phi (\sin\omega)^{m+e-1}(\cos\omega)^{n-e} \, d\omega, \qquad n = 5.$$

In (9) "=" holds if there is no local or global self-overlap of the tube, and "$\leq$" holds when there is no local self-overlap.

The constant κ_0 is the volume of the manifold Γ and in the case of the Gaussian kernel is easily found to be

$$|\Gamma| = \int_{C\times Q^*} \|g\|^{1/2} \, d\mathbf{t}\, d\theta\, d\sigma\, dc = \frac{\pi|C|}{16}\left(\frac{1}{\sigma_1^2} - \frac{1}{\sigma_2^2}\right)\left(\frac{1}{2}\left(\frac{1}{c_2^2} - \frac{1}{c_1^2}\right) + \log\frac{c_2}{c_1}\right).$$

The constant κ_2 is given by

$$\kappa_2 = \int_{C\times Q^*} \left(-\frac{S}{2} - \frac{n(n-1)}{2}\right)\|g\|^{1/2} \, d\mathbf{t}\, d\theta\, d\sigma\, dc, \qquad n = 5,$$

where S is the scalar curvature of the manifold Γ [see, e.g., Willmore (1959), pages 232 and 233], which can be calculated directly from the metric tensor. This expression for κ_2 and discussion of the algorithm appear in Sun (1993). It is interesting to note that as in the case of isotropic Gaussian kernel our manifold Γ has constant scalar curvature ($S = 18$) and hence $\kappa_2 = -19|\Gamma|$.

Assume now that the point z of the tube is one for which the closest point is γ^∂ from the part of the boundary $\partial\Gamma$ having a four-dimensional tangent space. In other words, we consider the point z to which the closest point is the point from the union of images of the sets $\partial C_s \times (0,\pi] \times (\sigma_1,\sigma_2) \times (c_1,c_2)$, $C \times (0,\pi] \times \{\sigma_1,\sigma_2\} \times (c_1,c_2)$, $C \times (0,\pi] \times (\sigma_1,\sigma_2) \times \{c_1,c_2\}$. Here ∂C_s denotes a smooth part of the boundary ∂C. We will use the notation $T_{\partial\Gamma}(\phi)$ for this part of the tube. Since calculations for manifolds with boundary do not appear in Weyl (1939), we will give more details for the general calculations and then present some examples specific to our problem. See Knowles and Siegmund (1989) for the case of a two-dimensional surface and Naiman (1990) for the case of the manifold that is the image of a convex polyhedron.

Points $z \in T_{\partial\Gamma}(\phi)$ can be represented as $z = y/\|y\|$, where

$$y = y(u_1,u_2,u_3,u_4,\eta,\xi_1,\ldots,\xi_{d-6}) = \gamma^\partial + \eta N + \xi_1 n(1) + \cdots + \xi_{d-6} n(d-6),$$

$\|y\| = (1 + \eta^2 + \sum_{i=1}^{d-6}\xi_i^2)^{1/2}$, and the quadruple $\mathbf{u} = (u_1,u_2,u_3,u_4)$ denotes the coordinates parameterizing one of the parts of the boundary described above. The particular choice of the parameterization for each part will be described below. The normal N is a vector in the tangent space of Γ, but orthogonal to the boundary and pointing into the manifold, so that $\eta \leq 0$. The volume element is

$$dV_{\partial\Gamma}(z) = \|y, y_1, y_2, y_3, y_4, N, n(1), \ldots, n(d-6)\| \frac{du\, d\eta\, d\xi_1 \cdots d\xi_{d-6}}{(1 + \eta^2 + \sum_{i=1}^{d-6}\xi^2)^{d/2}},$$

where $y_i = \gamma_i^{\partial} + \eta N_i + \sum_{k=1}^{d-6} \xi_k n_i(k)$, $i = 1, \ldots, 4$, $\gamma_i^{\partial} = \partial\gamma^{\partial}/\partial u_i$, $n_i(k) = \partial n(k)/\partial u_i$, $N_i = \partial N/\partial u_i$. By extending the Weingarten map [cf. Millman and Parker (1977), page 125] to manifolds of dimension greater than 2, $n_i(k)$ and N_i can be expressed as a linear combination of γ^{∂}, γ_i^{∂}, $i = 1, \ldots, 4$, and N, $n(k)$, $k = 1, \ldots, d-6$, as

$$N_i = -\sum_{j=1}^{4} G_i^j \gamma_j^{\partial} + \cdots,$$

$$n_i(k) = -\sum_{j=1}^{4} L_i^j(k) \gamma_j^{\partial} + \cdots,$$

where $+\cdots$ denotes the part of the expansion orthogonal to the tangent space spanned by the γ_i^{∂}, $i = 1, \ldots, 4$. Along the lines of Knowles and Siegmund (1989), we get

$$dV_{\partial\Gamma}(z) = \|g^{\partial}\|^{1/2} \left\| I - \eta G - \sum_{k=1}^{d-6} \xi_k L(k) \right\| \frac{d\mathbf{u}\, d\eta\, d\xi_1 \cdots d\xi_{d-6}}{(1 + \eta^2 + \sum_{k=1}^{d-6} \xi_k^2)^{d/2}},$$

where $G = (G_i^j)_{j,i=1}^4$, $L(k) = (L_i^j(k))_{j,i=1}^4$ and g^{∂} is the metric tensor of the manifold $\partial\Gamma$. The volume of this part of the tube is

$$V_{\partial\Gamma}(\phi) = \int_{\partial\Gamma} \int_{\sum_{k=1}^{d-6} \xi_k^2 + \eta^2 \le \tan^2\phi, \eta \le 0} \left\| I - \eta G - \sum_{k=1}^{d-6} \xi_k L(k) \right\| \times \frac{d\eta\, d\xi_1 \cdots d\xi_{d-6}}{(1 + \eta^2 + \sum_{k=1}^{d-6} \xi_k^2)^{d/2}}\, dA_{\partial\Gamma},$$

where $dA_{\partial\Gamma}$ is the volume element of the boundary $\partial\Gamma$. We expand the determinant and integrate to obtain

$$V_{\partial\Gamma}(\phi) = \tfrac{1}{2}\omega_{d-6}\kappa_0^{\partial} J_0^{\partial}(\phi) + \omega_{d-7} J_2(\phi)\kappa_1^{\partial} + o\big(J_2(\phi)\big), \qquad \phi \to 0, \tag{10}$$

where κ_0^{∂} is the volume of the boundary, κ_1^{∂} is the integrated geodesic mean curvature of the boundary [cf. Siegmund and Worsley (1995)], and we have assumed there is no self-overlap.

Elements of the matrix of the Weingarten map, $(G_i^j)_{j,i=1}^4$, can be found in the following way. From the Weingarten equations

$$\frac{\partial N}{\partial u_i} = -\sum_{j=1}^{4} G_i^j \gamma_j^{\partial} + \cdots$$

and the simple fact that

$$\frac{\partial}{\partial u_i}\langle N, \gamma_j^{\partial}\rangle = 0 = \left\langle \frac{\partial N}{\partial u_i}, \gamma_j^{\partial} \right\rangle + \langle N, \gamma_{ji}^{\partial}\rangle,$$

it follows that for each fixed i vector $(G_i^j)_{j=1}^4$ is the solution of a system of linear equations

$$\langle N, \gamma_{ik}^{\partial} \rangle = \sum_{j=1}^{4} G_i^j g_{jk}^{\partial}, \qquad k = 1, 2, 3, 4.$$

Below we present examples of calculations of κ_0^{∂} and κ_1^{∂} for different parts of the boundary $\partial\Gamma$.

$\partial\Gamma_\sigma = \gamma : C \times [0, \pi] \times \{\sigma_1, \sigma_2\} \times (c_1, c_2) \to \mathbb{R}^d$. Here $\mathbf{u} = (t_1, t_2, \theta, c)$ and $\gamma^{\partial}(\mathbf{u}) = \gamma(t_1, t_2, \theta, \sigma_i, c)$, $i = 1, 2$. First, we find the unit normal to $\partial\Gamma_\sigma$, which lies in the tangent space of Γ, that is, is a linear combination of vectors $\gamma_{\mathbf{t}}, \gamma_\theta, \gamma_\sigma, \gamma_c$ and orthogonal to the tangent space generated by $\gamma_{\mathbf{t}}, \gamma_\theta, \gamma_c$. It can be seen that the vector γ_σ is orthogonal to all but γ_c, and "one-step" Gram–Schmidt orthogonalization gives the unit normal

$$N = 2^{1/2}(\sigma\gamma_\sigma - c\gamma_c),$$

which points into the manifold Γ at $\sigma = \sigma_1$ and outward at $\sigma = \sigma_2$.

The metric tensor for $\partial\Gamma_\sigma$ is easily derived from the expression for g given above, and

$$\kappa_0^{\partial} = \sum_{i=1}^{2} |\partial\Gamma_{\sigma_i}| = \frac{\pi|C|}{8\sqrt{2}} \left(\frac{1}{\sigma_1^2} + \frac{1}{\sigma_2^2} \right) \left(2 \log \frac{c_2}{c_1} + \frac{1}{c_2^2} - \frac{1}{c_1^2} \right).$$

The integrated boundary curvature κ_1^{∂} can be found from the following system (which is relatively simple due to the block-diagonal form of the metric tensor g^{∂}):

$$\begin{aligned}
\langle N, \gamma_{t_1 t_1} \rangle &= G_1^1 a_{11}/2 + G_1^2 a_{12}/2, \\
\langle N, \gamma_{t_1 t_2} \rangle &= G_1^1 a_{12}/2 + G_1^2 a_{22}/2, \\
\langle N, \gamma_{t_2 t_2} \rangle &= G_2^2 a_{22}/2 + G_2^1 a_{12}/2, \\
\langle N, \gamma_{t_2 t_1} \rangle &= G_2^2 a_{12}/2 + G_2^1 a_{11}/2, \\
\langle N, \gamma_{\theta\theta} \rangle &= G_3^3 (c^2 - 1)^2/(4c^2), \\
\langle N, \gamma_{cc} \rangle &= G_4^4/(2c^2).
\end{aligned}$$

Calculation of $\langle N, \gamma_{u_i u_j} \rangle$ involves evaluation of expressions of the form $\langle \gamma_{u_i u_j}, \gamma_\sigma \rangle$, $\langle \gamma_{u_i u_j}, \gamma_c \rangle$. One way to do this is to calculate the corresponding derivatives of the covariance function. Another way is to use the "cyclic permutation of indices" technique often used in differential geometry, which allows one to calculate the values of interest directly from the metric tensor of the manifold Γ. It is especially simple to apply here due to the relative simplicity of the metric tensor. Below we present one example of such calculation, say for $\langle \gamma_{t_1 t_2}, \gamma_c \rangle$.

EXAMPLE.

$$\partial g_{t_1c}/\partial t_2 = 0 = \langle \gamma_{t_1t_2}, \gamma_c \rangle + \langle \gamma_{t_1}, \gamma_{ct_2} \rangle,$$

$$\partial g_{t_2c}/\partial t_1 = 0 = \langle \gamma_{t_1t_2}, \gamma_c \rangle + \langle \gamma_{t_2}, \gamma_{ct_1} \rangle,$$

$$\partial g_{t_1t_2}/\partial c = \sigma^{-2}c^{-3}\sin\theta\cos\theta = \langle \gamma_{t_1}, \gamma_{ct_2} \rangle + \langle \gamma_{t_2}, \gamma_{ct_1} \rangle = 2\langle \gamma_{t_1}, \gamma_{ct_2} \rangle,$$

which implies $\langle \gamma_{t_1t_2}, \gamma_c \rangle = -\langle \gamma_{t_1}, \gamma_{ct_2} \rangle = -0.5\sigma^{-2}c^{-3}\sin\theta\cos\theta$.

Using the results of these calculations and solving the system of linear equations given above, we arrive at the following expression for the curvature of the boundary at σ_i:

$$\sum_{j=1}^{4} G_j^j = (-1)^{i+1} 2\sqrt{2}c^2/(c^2-1), \qquad i = 1, 2,$$

and

$$\kappa_1^{\partial} = \frac{|C|\pi}{2}\left(\frac{1}{\sigma_1^2} - \frac{1}{\sigma_2^2}\right)\log\frac{c_2}{c_1}.$$

Now let $\partial\Gamma_c = \gamma : C \times [0, \pi] \times (\sigma_1, \sigma_2) \times \{c_1, c_2\} \to \mathbb{R}^d$. Here $\mathbf{u} = (t_1, t_2, \theta, \sigma)$ and $\gamma^{\partial}(\mathbf{u}) = \gamma(t_1, t_2, \theta, \sigma, c_i)$, $i = 1, 2$. For this part of the boundary, the unit normal $N = 2c\gamma_c - \sigma\gamma_\sigma$,

$$\kappa_0^{\partial} = \frac{\pi|C|}{8}\left(\frac{1}{\sigma_1^2} - \frac{1}{\sigma_2^2}\right)\left(1 - \frac{1}{c_1^2} + 1 - \frac{1}{c_2^2}\right)$$

and

$$\kappa_1^{\partial} = \frac{\pi|C|}{4}\left(\frac{1}{\sigma_1^2} - \frac{1}{\sigma_2^2}\right)\left(\frac{1}{c_2^2} - \frac{1}{c_1^2}\right).$$

REMARK. For the case $c_1 = 1$, where we consider the boundary at c_2 only, we find that κ_0^{∂} is as given above with $c_1 = 1$, but surprisingly $\kappa_1^{\partial} = (\pi|C|/4)(1/\sigma_1^2 - 1/\sigma_2^2)(1 + 1/c_2^2)$. This is the source of one half the recommended modification of (8) when $c_1 = 1$. (The other half comes from addition of the scale space term to account for the singularity in the manifold at $c_1 = 1$.)

More complicated calculations arise when we consider $\partial\Gamma_{\partial C_s} = \gamma : \partial C_s \times [0, \pi] \times (\sigma_1, \sigma_2) \times (c_1, c_2) \to \mathbb{R}^d$. Initially, assume for simplicity that ∂C is a smooth closed curve. To calculate the volume of $\partial\Gamma_{\partial C_s}$, it is convenient to parameterize ∂C in terms of its arc length s starting from some fixed point on ∂C. Let $\tau(s) = (\tau_1(s), \tau_2(s))$ be such parameterization. Then $\mathbf{u} = (s, \theta, \sigma, c)$ and $\gamma^{\partial}(\mathbf{u}) = \gamma(\tau_1(s), \tau_2(s), \theta, \sigma, c)$. The metric tensor has the form

$$g^{\partial} = \begin{bmatrix} \dot{\tau}'\mathbf{A}\dot{\tau}/2 & 0 & 0 & 0 \\ 0 & (c^2-1)^2/(4c^2) & 0 & 0 \\ 0 & 0 & 1/\sigma^2 & 1/(2\sigma c) \\ 0 & 0 & 1/(2\sigma c) & 1/(2c^2) \end{bmatrix},$$

and

$$\kappa_0^{\partial} = |\partial\Gamma_{\partial C_s}|$$
$$= \int_0^{\pi}\int_{\sigma_1}^{\sigma_2}\int_{c_1}^{c_2}\int_0^{|\partial C|} \frac{c^2-1}{4\sqrt{2}c^2\sigma}\left\{\begin{pmatrix}\dot\tau_1(s)\\ \dot\tau_2(s)\end{pmatrix}'\mathbf{A}\begin{pmatrix}\dot\tau_1(s)\\ \dot\tau_2(s)\end{pmatrix}\right\}^{1/2} ds\,d\theta\,d\sigma\,dc.$$

Since $\tau(s)$ is a unit speed curve, we can write $(\dot\tau_1(s), \dot\tau_2(s)) = (\cos\alpha(s), \sin\alpha(s))$ for some differentiable function $\alpha(s)$, where $\alpha(0) \in [0, 2\pi)$. Then the expression for κ_0^{∂} can be rewritten as

$$|\partial\Gamma_{\partial C}| = \int_0^{\pi}\int_{\sigma_1}^{\sigma_2}\int_{c_1}^{c_2}\int_0^{|\partial C|} \frac{c^2-1}{4\sqrt{2}c^2\sigma}\Big(\frac{\cos^2(\alpha(s)-\theta)}{\sigma^2} + \frac{\sin^2(\alpha(s)-\theta)}{\sigma^2c^2}\Big)^{1/2} ds\,d\theta\,d\sigma\,dc$$
$$= \int_{\sigma_1}^{\sigma_2}\int_{c_1}^{c_2}\int_0^{|\partial C|}\int_{\alpha(s)-\pi}^{\alpha(s)} \frac{c^2-1}{4\sqrt{2}c^2\sigma^2}\Big(\cos^2\phi + \frac{\sin^2\phi}{c^2}\Big)^{1/2} ds\,d\phi\,d\sigma\,dc$$
$$= \frac{|\partial C|}{2\sqrt{2}}\Big(\frac{1}{\sigma_1} - \frac{1}{\sigma_2}\Big)\int_{c_1}^{c_2} \frac{c^2-1}{c^2}\mathrm{E}\Big(\Big[\frac{c^2-1}{c^2}\Big]^{1/2}\Big)\,dc.$$

Here, as before, $\mathrm{E}(y)$ is a complete elliptic integral of the second kind. It is easy to see that this result holds for any ∂C that is a union of piecewise regular curves.

To calculate the geodesic curvature, we assume for now that ∂C is smooth and, for example, parameterized by its arc length. The tangent space of $\partial\Gamma_{\partial C}$ is spanned by $\dot\tau_1(s)\gamma_{t_1} + \dot\tau_2(s)\gamma_{t_2}, \gamma_\theta, \gamma_\sigma, \gamma_c$. It is easy to see that the corresponding unit normal can be expressed as a linear combination of γ_{t_1}, γ_{t_2}, say $N = C_1(s,\theta,\sigma,c)\gamma_{t_1} + C_2(s,\theta,\sigma,c)\gamma_{t_2}$, the explicit form of which does not interest us now. For the elements of $(G_i^j)_{i=1}^4$, we can derive a system of linear equations analogous to the one considered above. The following observation simplifies the task. By noticing that $\langle\gamma_\theta, \gamma_{t_i}\rangle = \langle\gamma_\sigma, \gamma_{t_i}\rangle = \langle\gamma_c, \gamma_{t_i}\rangle = 0$, $i = 1, 2$, and $\langle\gamma_\sigma, \gamma_\sigma\rangle, \langle\gamma_\sigma, \gamma_c\rangle, \langle\gamma_c, \gamma_c\rangle, \langle\gamma_\theta, \gamma_\theta\rangle$ do not depend on t_i, $i = 1, 2$, and by differentiating, one can see that $\langle\gamma_{\theta\theta}, \gamma_{t_i}\rangle = \langle\gamma_{\sigma\sigma}, \gamma_{t_i}\rangle = \langle\gamma_{cc}, \gamma_{t_i}\rangle = \langle\gamma_{\sigma c}, \gamma_{t_i}\rangle = 0$.

This discussion leads to the conclusion that all but one diagonal entry of the Weingarten map are 0. The nonzero entry arises from $\langle\gamma_{ss}^{\partial}, N\rangle = G_1^1 g_{11}^{\partial}$, where g_{11}^{∂} was written explicitly above. So

$$\kappa_1^{\partial} = \int_0^{\pi}\int_{c_1}^{c_2}\int_{\sigma_1}^{\sigma_2} \frac{c^2-1}{4c^2\sigma}\int_0^{|\partial C|} \langle\gamma_{ss}^{\partial}, N\rangle \frac{1}{(g_{11}^{\partial})^{1/2}}\,ds\,d\sigma\,dc\,d\theta.$$

Now, for each fixed (θ, σ, c), the curve that is the image of ∂C can be parameterized in terms of its arc length t. For example, $t = t(s) = 2^{-1/2}\int_0^s [\dot\tau(v)' \times \mathbf{A}\dot\tau(v)]^{1/2}\,dv$ in the case that ∂C consists of a single smooth curve. Then

$$\tilde\gamma^{\partial}(\mathbf{u}) = \tilde\gamma^{\partial}(t,\theta,\sigma,c) = \gamma\big(\tau_1(s(t)), \tau_2(s(t)), \theta, \sigma, c\big),$$

and

$$\langle \gamma_{ss}^{\partial}, N\rangle = \langle \tilde{\gamma}_{tt}^{\partial}, N\rangle \left(\frac{dt}{ds}\right)^2 + \langle \tilde{\gamma}_{t}^{\partial}, N\rangle \left(\frac{d^2t}{ds^2}\right) = \langle \tilde{\gamma}_{tt}^{\partial}, N\rangle \left(\frac{dt}{ds}\right)^2.$$

The change of variables $s = s(t)$ leads to the innermost integral being seen to equal

$$\int_{\partial\Gamma_{\partial C}(\theta,\sigma,c)} \langle \tilde{\gamma}_{tt}^{\partial}, N\rangle \, dt,$$

where $\partial\Gamma_{\partial C}(\theta,\sigma,c)$ is the boundary of the surface $\gamma(\mathbf{t},\theta,\sigma,c)$ considered as a function of $\mathbf{t}$ and $\langle \tilde{\gamma}_{tt}^{\partial}, N\rangle$ is the geodesic curvature of this boundary. Since the entries of the metric tensor of the surface do not depend on $\mathbf{t}$, the Gaussian curvature of the corresponding surface is 0, and the Gauss–Bonnet theorem shows that $\int_{\partial\Gamma_{\partial C}(\theta,\sigma,c)} \langle \tilde{\gamma}_{tt}^{\partial}, N\rangle \, dt$ is equal to the Euler characteristic of C multiplied by 2π. Finally, we get

$$\kappa_1^{\partial} = \frac{2\pi\chi(C)}{4}\pi \log\frac{\sigma_2}{\sigma_1}\left(c_2 - c_1 + \frac{1}{c_2} - \frac{1}{c_1}\right).$$

Following the same scheme as above, one could obtain results for the part of the tube arising from the $\partial^2\Gamma$, that is, the "angles" of the boundary, which in our case are the images of the following sets: $C \times [0,\pi] \times \{\sigma_1,\sigma_2\} \times \{c_1,c_2\}$, $\partial C_s \times [0,\pi] \times \{\sigma_1,\sigma_2\} \times (c_1,c_2)$, $\partial C_s \times [0,\pi] \times (\sigma_1,\sigma_2) \times \{c_1,c_2\}$, $\partial^2 C \times [0,\pi] \times (\sigma_1,\sigma_2) \times (c_1,c_2)$. Here $\partial^2 C$ stands for the vertices of ∂C (exterior angles of ∂C are assumed to be positive).

For the point z of the tube to which the closest point is γ^{∂^2} from $\partial^2\Gamma (z \in T_{\partial^2\Gamma}(\phi))$, we have $z = y/\|y\|$, where

$$\begin{aligned} y &= y(u_1,u_2,u_3,\eta_1,\eta_2,\xi_1,\ldots,\xi_{d-6}) \\ &= \gamma^{\partial^2} + \eta_1 N(1) + \eta_2 N(2) + \xi_1 n(1) + \cdots + \xi_{d-6} n(d-6), \end{aligned}$$

$\|y\| = (1 + \eta_1^2 + 2\zeta\eta_1\eta_2 + \eta_2^2 + \sum_{i=1}^{d-6}\xi_i^2)^{1/2}$, $\eta_1, \eta_2 \le 0$. Here $N(1)$, $N(2)$ are the unit vectors lying in the tangent space of Γ and normal to the tangent spaces of the parts of the boundary $\partial\Gamma$ the intersection of which constitutes the corresponding part of $\partial^2\Gamma$, and $\zeta = \langle N(1), N(2)\rangle$ (assume that $|\zeta| < 1$). Weingarten equations in this case take the form $N_i(k) = -\sum_{j=1}^{3} G_i^j(k)\gamma_j^{\partial^2} + \cdots$, $k = 1,2$, $n_i(k) = -\sum_{j=1}^{3} L_i^j(k)\gamma_j^{\partial^2} + \cdots$, $k = 1,\ldots,d-6$, $G(k) = (G_i^j(k))_{j,i=1}^3$, $L(k) = (L_i^j(k))_{j,i=1}^3$.

REMARK. In the representation of z, we implicitly assumed that $N(1)$ and $N(2)$ are linearly independent, although this is not necessarily the case. For example, in our problem it can happen that the boundary ∂C has vertices where the tangent rotates by π. More work is needed to deal with these cases, which we exclude from our consideration.

Omitting a few steps in the derivation of the volume of $T_{\partial^2\Gamma}(\phi)$, we have

$$V_{\partial^2\Gamma}(\phi) = J_2(\phi)\omega_{d-7}\kappa_0^{\partial^2} + o\big(J_2(\phi)\big), \qquad \phi \to 0. \tag{11}$$

To evaluate (11), we must find the angle between the corresponding unit normals $N(1)$, $N(2)$. It is easy to see that $N(1) \perp N(2)$ and $\arccos(\zeta) = \pi/2$ for the parts of $\partial^2\Gamma$ that are the images of $\partial_s C \times [0,\pi) \times \{\sigma_1,\sigma_2\} \times (c_1,c_2)$, $\partial_s C \times [0,\pi] \times (\sigma_1,\sigma_2) \times \{c_1,c_2\}$. For the image of $C \times [0,\pi] \times \{\sigma_1,\sigma_2\} \times \{c_1,c_2\}$, it is easy to see from the previous calculations that $\langle N(1), N(2)\rangle = -1/2^{1/2}$, $\arccos(\zeta) = 3\pi/4$ for $(\sigma,c) = (\sigma_i,c_i)$, $i = 1,2$; and $\langle N(1), N(2)\rangle = 1/2^{1/2}$, $\arccos(\zeta) = \pi/4$ for $(\sigma,c) = (\sigma_i,c_j)$, $i,j = 1,2$, $i \neq j$. In the case that $\partial^2\Gamma$ is the image of $\partial^2 C \times [0,\pi] \times (\sigma_1,\sigma_2) \times (c_1,c_2)$ for each vertex and fixed θ, σ, c, $\arccos(\zeta)$ is just the angle of rotation of the tangent to the boundary of the two-dimensional surface $\gamma(\mathbf{t},\theta,\sigma,c)$ considered as a function of $\mathbf{t}$. So, for the part of the boundary which is the image of $\partial C \times [0,\pi] \times (\sigma_1,\sigma_2) \times (c_1,c_2)$, we can combine the above result with the integral appearing in the derivation of the expression for κ_1^{∂} to get

$$\int_{\partial\Gamma_{\partial C}(\theta,\sigma,c)} \langle \tilde{\gamma}_{tt}^{\partial}, N\rangle\, dt + \sum_{i=1}^{V} \arccos(\zeta_i) = 2\pi\chi(C),$$

which again follows from the Gauss–Bonnet theorem. In this equation, V is the number of vertices, and the integral should be understood as a sum over smooth parts of the boundary. As a result, the total input from the curvature of the part of the boundary under consideration and "angles" is equal to $\omega_{d-7}J_2(\phi)\kappa_1^{\partial}$, where κ_1^{∂} was defined earlier.

Now we can combine (9), (10) and (11) to obtain as $\phi \to 0$ the expansion

$$\begin{aligned} V_\Gamma(\phi) = {} & \omega_{d-7}\kappa_0 J_0(\phi) + 0.5\omega_{d-6}\kappa_0^{\partial} J_0^{\partial}(\phi) \\ & + \omega_{d-7}\big(\kappa_2 + \kappa_1^{\partial} + \kappa_0^{\partial^2}\big)J_2(\phi) + o\big(J_2(\phi)\big). \end{aligned}$$

Putting these expressions together as in Knowles and Siegmund (1989) or Sun (1993), we obtain

$$\begin{aligned} & P\left\{ \max_{(\mathbf{t},\theta,\sigma,c)\in C\times Q^*} X(\mathbf{t},\theta,\sigma,c) \geq x \right\} \\ & \quad = \phi(x)x^4(2\pi)^{-5/2}\kappa_0 + \phi(x)x^3 0.5(2\pi)^{-2}\kappa_0^{\partial} \\ & \qquad + \phi(x)x^2(2\pi)^{-5/2}\big(4\kappa_0 + \kappa_2 + \kappa_1^{\partial} + \kappa_0^{\partial^2}\big) + o\big(x^2\phi(x)\big), \qquad x \to \infty, \end{aligned}$$

and hence display (8).

Acknowledgments. The authors thank Alan Evans and Malk Wolforth of the Montreal Neurological Institute for permission to use the fMRI data.

REFERENCES

ABRAMOWITZ, M. and STEGUN, I. A. (1964). *Handbook of Mathematical Functions*. National Bureau of Standards, Washington, DC.

ADLER, R. J. (1981). *The Geometry of Random Fields*. Wiley, New York.

ADLER, R. J. (2000). On excursion sets, tube formulae, and maxima of random fields. *Ann. Appl. Probab.* **10** 1–74.

ADLER, R. J. and HASOFER, A. M. (1976). Level crossing for random fields. *Ann. Probab.* **4** 1–12.

DAUBECHIES, I. (1992). *Ten Lectures on Wavelets.* SIAM, Philadelphia.

GOTT, J., PARK, C., JUSKIEWICZ, R., BIES, W., BENNETT, D., BOUCHET, F. R. and STEBBINS, A. (1990). Topology of microwave background fluctuations: Theory. *Astrophysical J.* **352** 1–14.

HOTELLING, H. (1939). Tubes and spheres in n-space and a class of statistical problems. *Amer. J. Math.* **61** 440–460.

KNOWLES, M. and SIEGMUND, D. (1989). On Hotelling's approach to testing for a nonlinear parameter in regression. *Internat. Statist. Rev.* **57** 205–220.

KWONG, K., BELLIVEAU, J., CHESLER, D., GOLDBERG, I., WEISSKOFF, R., PONCELET, B., KENNEDY, D., HOPPEL, B., COHEN, M., TURNER, R., CHENG, H.-M., BRADY, T. and ROSEN, B. (1992). Dynamic magnetic resonance imaging of human brain activity during primary sensory stimulation. *Proc. Nat. Acad. Sci. U.S.A.* **89** 5675–5679.

LINDEBERG, T. (1994). *Scale-Space Theory in Computer Vision*. Kluwer, Boston.

MILLMAN, R. S. and PARKER, G. D. (1977). *Elements of Differential Geometry*. Prentice-Hall, Englewood Clifts, NJ.

NAIMAN, D. Q. (1990). Volumes of tubular neighborhoods of spherical polyhedra and statistical inference. *Ann. Statist.* **18** 685–716.

OUYANG, X., PIKE, G. and EVANS, A. (1994). fmri of human visual cortex using temporal correlation and spatial coherence analysis. In *13th Annual Symposium of the Society for Magnetic Resonance in Medicine*.

POLINE, J.-B. and MAZOYER, B. (1994). Enhanced detection in brain activation maps using a multifiltering approach. *J. Cerebral Blood Flow and Metabolism* **14** 639–642.

RABINOWITZ, D. (1994). Detecting clusters in disease incidence. In *Change-Point Problems* (E. G. Carlstein, H.-G. Müller and D. Siegmund, eds.) 255–275. IMS, Hayward, CA.

SEARLE, S. R. (1982). *Matrix Algebra Useful for Statistics*. Wiley, New York.

SHAFIE, K. (1998). The geometry of Gaussian rotation space random fields. Ph.D. dissertation, Dept. Mathematics and Statistics, McGill Univ., Montreal. Available at www.math.mcgill.ca/shafie.

SIEGMUND, D. O. and WORSLEY, K. J. (1995). Testing for a signal with unknown location and scale in a stationary Gaussian random field. *Ann. Statist.* **23** 608–639.

SIEGMUND, D. and ZHANG, H. (1993). The expected number of local maxima of a random field and the volume of tubes. *Ann. Statist.* **21** 1948–1966.

SIGAL, S. (1998). Detection of a smooth signal in fixed sample and sequential problems. Ph.D. dissertation, Dept. Statistics, Stanford Univ.

SUN, J. (1993). Tail probabilities of the maxima of Gaussian random fields. *Ann. Probab.* **21** 34–71.

TAKEMURA, A. and KURIKI, S. (2002). On the equivalence of the tube and Euler characteristic methods for the distribution of the maximum of Gaussian fields over piecewise smooth domains. *Ann. Appl. Probab.* **12** 768–796.

WEYL, H. (1939). On the volume of tubes. *Amer. J. Math.* **61** 461–472.

WILLMORE, T. J. (1959). *An Introduction to Differential Geometry*. Oxford Univ. Press.

WORSLEY, K. J. (1994). Local maxima and the expected Euler characteristic of excursion sets of χ^2, F and t fields. *Adv. in Appl. Probab.* **26** 13–42.

WORSLEY, K. J. (2001). Testing for signals with unknown location and scale in a χ^2 random field, with an application to fMRI. *Adv. in Appl. Probab.* **33** 773–793.

WORSLEY, K., EVANS, A., MARRETT, S. and NEELIN, P. (1992). A three-dimensional statistical analysis for cbf activation studies in human brain. *J. Cerebral Blood Flow and Metabolism* **12** 900–918.

K. SHAFIE
DEPARTMENT OF STATISTICS
FACULTY OF MATHEMATICAL SCIENCES
SHAHID BEHESHTI UNIVERSITY
EVEEN, TEHRAN
IRAN
E-MAIL: k-shafie@cc.sbu.ac.ir

B. SIGAL
DEPARTMENT OF RADIOLOGY
STANFORD UNIVERSITY
STANFORD, CALIFORNIA
E-MAIL: slava@stanford.edu

D. SIEGMUND
DEPARTMENT OF STATISTICS
STANFORD UNIVERSITY
STANFORD, CALIFORNIA
E-MAIL: dos@stat.stanford.edu

K. J. WORSLEY
DEPARTMENT OF MATHEMATICS
AND STATISTICS
MCGILL UNIVERSITY
MONTREAL, QUEBEC
CANADA H3A 2K6
E-MAIL: keith@math.Mcgill.ca